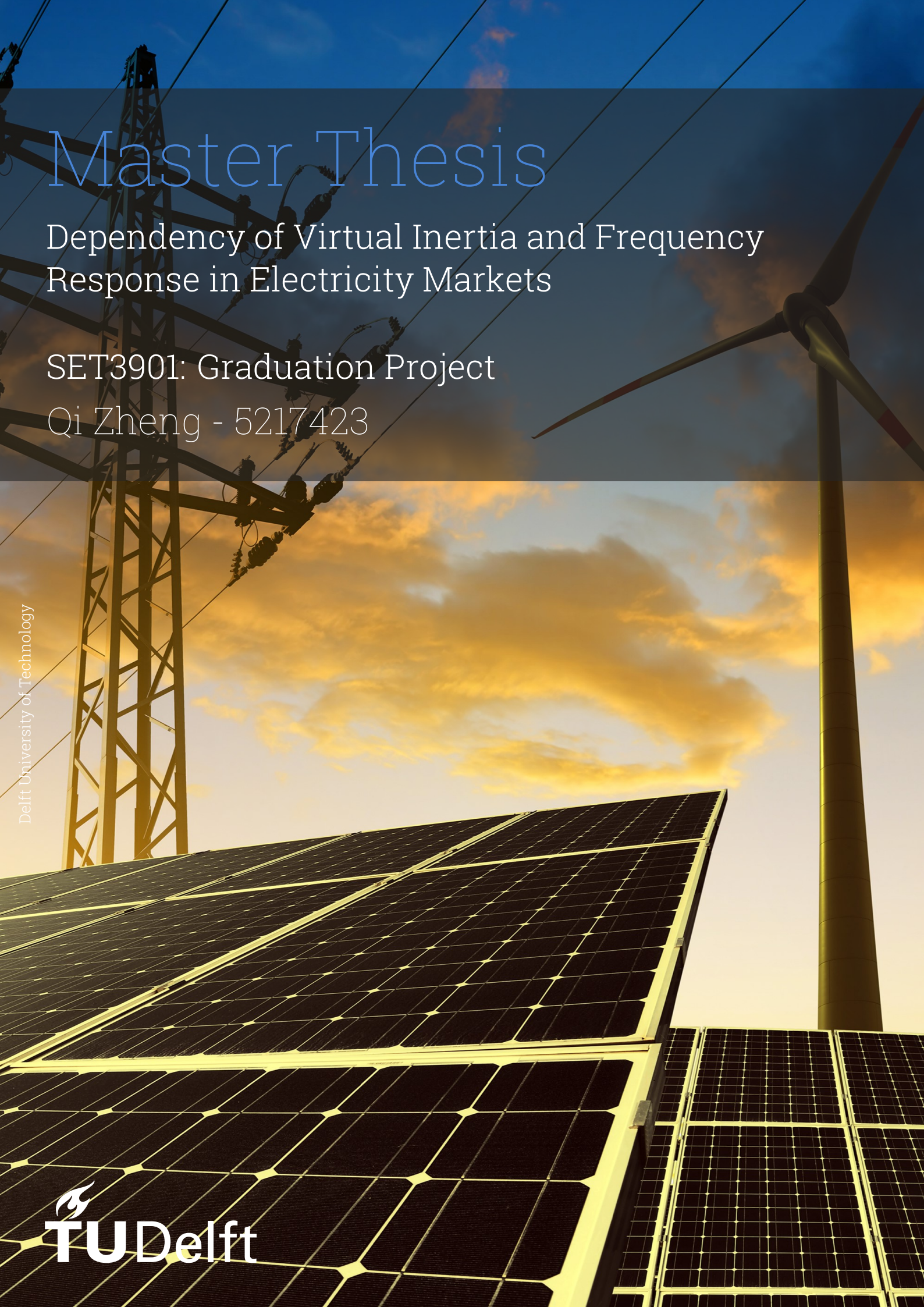

Master Thesis

Dependency of Virtual Inertia and Frequency Response in Electricity Markets

SET3901: Graduation Project

Qi Zheng - 5217423

Delft University of Technology

TU Delft

Master Thesis

Dependency of Virtual Inertia and Frequency Response in Electricity Markets

by

Qi Zheng - 5217423

to obtain the degree of Master of Science
at the Delft University of Technology,
to be defended publicly on Thursday the 30 November 2023 at 08:45

Student number:	5217423	
Project duration:	1 December 2022 - 30 November 2023	
Thesis committee:	Prof. L.J. de Vries	Thesis advisor
	Dr. J. L. Cremer	Thesis supervisor
	H. Xie	Thesis supervisor
	V. Zobernig	Thesis supervisor

TU Delft

Preface

This report is part of the thesis project for the Master of Science in Sustainable Energy Technology (MSc SET) program at TU Delft. During the project, my daily supervisors Haiwei Xie and Viktor Zobernig gave generous recommendations throughout the scoping and literature review process and provided valuable feedback and encouragement till the end of the project. The project would not be possible without their continuous support. My thesis supervisor Jochen Cremer gave a lot of important advice on research methodology and the choice of research focus. Laurens de Vries helped me understand some common fallacies when doing a project so that I can avoid them.

I would also like to express my gratitude to other people in the research group, especially Mert Karaçelebi, who kindly gave suggestions during the weekly update meetings. It was a bit of luck to be with the guys in the study room who gave me advice, motivation, and friendship throughout the study at TU Delft.

Finally, I would like to thank my parents, who made it possible for me to study abroad and provided countless help in my life and study.

Qi Zheng - 5217423
Delft, November 2023

Summary

In the electricity system, one barrier to the energy transition is the degradation of frequency stability due to the decrease of system inertia and frequency control ancillary services (FCAS), which is caused by the replacement of inertia-abundant and governor-based conventional power plants with zero-inertia and inverter-based renewable energy sources (RES).

There are already inverter technologies for RES and battery energy storage systems (BESS) to provide virtual inertia (VI) and fast frequency response (FFR) services, which are equivalent to physical inertia and conventional FCAS. Potential providers include wind, solar, battery energy storage systems (BESS), and other types of devices with the feature of energy storage. However, there are non-technical barriers to the actual implementation. For example, in most parts of the world, these services cannot participate in the electricity market and thus there is a lack of incentive for both the provision of and investment in the VI and FFR.

In the literature, there are already proposals of possible market designs for VI and FFR that procure the services, guarantee the frequency-stability requirements, and provide payments to the service provider. The main focal point is on the formulation of security-constrained unit commitment (SCUC) and security-constrained economic dispatch (SCED) problems. The formulation needs to be accurate in modeling, be solvable, and be with reasonable computational burden. Most of them only considered the allocation of ancillary services but did not price them, or price them but only by directly assigning a shadow price. Only a few works considered explicit prices in the bid.

In this project, we consider a market design with explicit bid prices. In the SCUC and SCED problems, we adopt the state-of-the-art formulation of frequency nadir constraint and method of modeling the frequency dynamics based on the linear ramp assumption of the dynamics of frequency response (FR). With these methodologies, we will investigate the features of such a market by identifying interdependencies of parameters in the market setups, including the interaction between the bid price and bid amount of FR and VI, and analyzing the underlying mechanisms. The results show that the amount of FR sold depends on the bid price of FR monotonously and the amount of VI sold depends on the bid price of VI monotonously, though with different patterns. The underlying reason for such dependencies is that FR, VI, and the size of the largest unit both help mitigate frequency drop and recover it and they are influencing each other. The price of FR or VI decides the relative worthiness of each option. The size of the largest unit is also related to the amount of FR sold, which is confirmed by the formulation of the analytical nadir and the QSS constraint. However, the way that the amount of available FR influences the amount of VI sold does not show a clear pattern.

These findings provide insights into the interactions between the FR and VI products and thus provide a reference for the design of the FCAS market.

Contents

Nomenclature

Abbreviations

Abbreviation	Definition
IPFR	Inertia and primary frequency response
GHG	Greenhouse gas
PFR	Primary frequency response
EFR	Enhanced frequency response
FR	Frequency response
RES	Renewable energy source
IBR	Inverter-based resource
VI	Virtual inetia
NEM	(Australia) National Electricity Market
UC	(Classic) unit commitment
ED	(Classic) economic dispatch
SCUC	Security-constrained unit commitment
SCED	Security-constrained economic dispatch
SUC	Stochastic unit commitment
LP	Linear programming
MILP	Mixed-integer linear programming
SOC	Second-order cone
SOCP	Second-order cone programming
SQP	Sequential quadratic programming
DAM	Day-ahead market
RTM	Real-time market
DR	Demand response

Abbreviation	Definition
CS	Consumer surplus
PS	Producer surplus
MSG	Minimum stable generation
UFLS	Under frequency load shedding
RoCoF	Rate of change of frequency
QSS	Quasi-steady state
PWL	Piece-wise linear
RTS	Reliability test system
KKT	Karush–Kuhn–Tucker (conditions)

Index

Symbol	Definition	Unit
k	Time step in dynamic simulation	[s]
t	Market periods	[h]
g	Generation units or FR provider	[-]
i	FR provider	[-]
j	VI provider	[-]

Sets

Symbol	Definition
K	A set of all dynamic simulation time steps
T	A set of all market periods

Symbol	Definition
G	A set of all generation units online
I	A set of all FR providers
J	A set of all VI providers

Parameters

Symbol	Definition	Unit
$\overline{P}_g$	Maximum active power of generator g	[p.u.]
$\underline{P}_g$	Minimum active power of generator g	[p.u.]
$P^{p.u.}$	Active power per unit	[MW]
d	Load	[p.u.]
H	Inertia constant	[s]
D	Load damping factor	[-]
R_g^{droop}	Droop constant of speed governor	[-]
T_1	Governor lag time constant	[t]
T_2	Turbine lead time constant	[t]
T_3	Turbine lag time constant	[t]
k^a	FR delay	[s]
k^b	FR delivery time	[s]
R_i	FR capacity	[p.u.]
dk	Step size of frequency dynamic simulation	[s]
f_0	Nominal frequency of the system	[Hz]
$\underline{\Delta\omega}$	Frequency nadir limit	[p.u.]
$\underline{\omega'}$	RoCoF limit	[p.u./s]
$\underline{\Delta}\omega_{qss}$		
c_g^{fix}	Fixed cost	[€/h]
c_g^{var}	Variable cost	[€/MWh]
$c_{t,i}^{fr}$	FR price	[€/MW-h]

Symbol	Definition	Unit
$c_{t,j}^{H}$	VI price	[€/MW-s]
k^{a}	Activation delay of FR	[s]
k^{b}	Time of full delivery of FR	[s]
$\overline{R}$	Bid amount of FR	[MW]
fr	Power injection from unit amount of FR	[-]
FR	Acumulated energy injection from unit amount of FR	[s]
$\overline{H_{vi}}$	Bid amount of VI	[MW-s]
J	Momentum of inertia of turbine	[kg-m^2]
T_m	Mechanical torque input	[N-m]
T_e	Electromagnetic torque input	[N-m]
δ	Angular position of rotor	[rad]
ω_m	Angular velocity of rotor	[rad/s]
$\omega_{m,0}$	Nominal angular velocity	[rad/s]
ω_{sys}	System frequency	[Hz]
P_m	Mechanical power input	[MW]
P_e	Electromagnatic power input	[MW]
S_{rated}	Apparent power	[MVA]
Δf_{max}	The absolute value of maximum allowed frequency deviation (frequency nadir limit) in the works by Badesa et. al	[Hz]
f_0	Nominal system frequency in the works by Badesa et. al	[Hz]
$y_{t,g}^{\star}$	The solution of commitment status of active power in the SCUC problem	[0/1]
$x_{t,g}^{\star}$	The solution of commitment status of FR product in the SCUC problem	[0/1]
$z_{t,g}^{\star}$	The solution of commitment status of VI product in the SCUC problem	[0/1]

Symbol	Definition	Unit
$P^{p.u.}$	Per unit active power	[MW]
P^{tot}	Total installed capacity	[MW]
$\omega^{p.u.}$	Per unit frequency	[Hz]

Decision variables, Objective Function, and Constraints

Symbol	Definition	Unit
$P_{t,g}$	Active Power	[p.u.]
$y_{t,g}$	Unit commitment status	[0/1]
P^L	The size of the largest dispatched active power (abbreviated as “the size of the largest unit)	[p.u.]
$R_{t,i}$	FR capacity	[p.u.]
$x_{t,i}$	FR commitment status	[0/1]
H_{vi}	VI capacity	[p.u.]
$z_{t,j}$	VI commitment status	[0/1]
J	Objective function	
P	The optimal value of primal problem	
D	The optimal value of the dual problem	
g^i	General symbol for inequality constraint with the name “i“	
h^i	General symbol for equality constraint with the name “i“	
Λ	General expression of dual variables	
X	General expression of primal variables	
L	Lagrangian (function)	
$\mathcal{L}$	Dual function	
$P_{g,t}^{c,v}$	Turbine valve position order (in the work by Xu et. al in 2016)	[MW]
$P_{g,t}^{c,r}$	Droop power order (in the work by Xu et. al in 2016)	[MW]

Symbol	Definition	Unit
$P_{g,t}^{c,x}$	Internal state of the lead-lag subsystem (in the work by Xu et. al in 2016)	[MW]
$P_{g,t}^{c,m}$	Mechanical power output (in the work by Xu et. al in 2016)	[MW]
π_H	Shadow price of inertia in the works by Badesa et. al	[€/MW-s]
π_{P^L}	Shadow price of reducing the size of the largest unit in the works by Badesa et. al	[€/MW]
π_R	Shadow price of frequecy response in the works by Badesa et. al	[€/MW]
μ	Dual value of the frequency nadir constraints in the works by Badesa et. al	[€/MW]

Linear expression of decision variables

Symbol	Definition	Unit
C^{fix}	Total fixed cost	[€]
C^{var}	Total variable cost	[€]
C^{fr}	Total FR payment	[€]
C^{H}	Total VI payment	[€]

1

Introduction

1.1. Background

Renewable energy in the electricity system is gaining momentum as a solution to climate change. More and more wind, solar, and other types of clean energy are introduced into the electricity system around the world at a fast pace to reduce greenhouse gas (GHG) emissions. For example, in Denmark, one of the forerunners in the area of the energy transition, the share of renewable energy sources (RES) in total installed capacity increased more than five times in the past two decades to almost 85% in 2022, as shown in Figure 1.1 [1]. In recent decades, this pattern will repeat in most other electricity systems around the world.

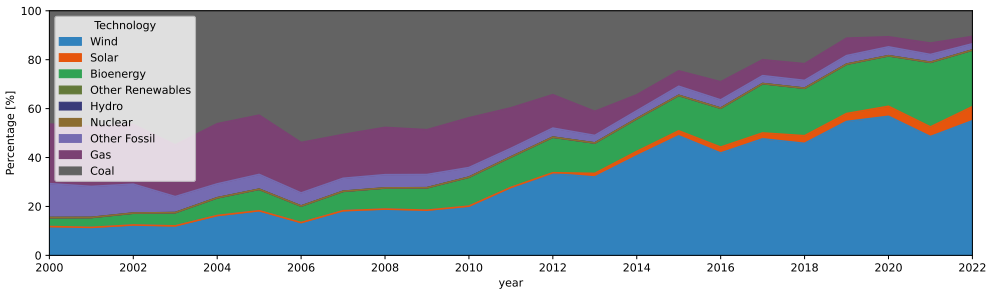

Figure 1.1: Share of RS in the Danish electricity system from the year 2000 to 2022. Data from [1]

The fast introduction of renewables imposes challenges to the power grid. For example, the variability of RES requires greater flexibility in the system; the uncertainty of RES requires more advanced forecasting tools; the uncontrollability of RES may result in curtailment; distributed renewables may cause network congestion and overheating of substation; the low marginal cost of RES will result in zero or even negative price in the electricity energy market, discouraging investments in power plants and bringing capacity adequacy into question [2].

Decreasing inertia and primary frequency control is one of the key challenges among others. Different from conventional power plants, RES, such as wind and solar, are connected to the power grid with inverters [3], and thus inverter-based resources (IBR) is another name for most variable RES. There is no physical inertia or frequency response (FR) from the speed governor in IBR, the total amount

of inertia and the capacity of primary frequency response (PFR) in the power grid will decrease with the increasing share of RES. As a result, the frequency stability will be compromised, especially after a contingency[1]. It has been recognized that, in some small regional systems, the estimated rate of change of frequency (RoCoF) after contingency is already too high to be safe during hours with high RES and low demand [4]. Extremely high RoCoF due to low inertia has already caused blackouts, for example in the South Australia grid on 28 September 2016, where the instantaneous share of RES at the moment was more than 50% [5]. With the increasing share of RES, the frequency stability issue will be more severe and frequent, and become a concern for bulk interconnected grids as well [6].

Virtual inertia (VI) and fast frequency response (FFR) are among the solutions to frequency stability issues in low-inertia grids. Even though IBRs contribute no physical inertia or PFR to the system, the technologies for IBRs to mimic the behavior of synchronous inertia and PFR of conventional generators are already mature, which are called VI or EFR, respectively [3, 7]. The controller algorithms of some IBRs can be designed in a way that the power injection is proportional to RoCoF, in the case of VI, or proportional to frequency deviation, in the case of FFR.

However, dedicated incentives are necessary to make sure that there are enough provisions for virtual inertia (VI) and frequency response (FR) in the low-inertia grid. FFR or equivalent products are only introduced to some regions, such as in the British, Irish, Australian, and New Zealand electricity markets as well as some parts of the US [8, 9]. Australian National Electricity Market (NEM) is a pioneer in the development of inertia products, but it is still under discussion [10]. Therefore, the way to provide incentives for VI and FR has been a meaningful research topic in recent decades.

Creating FR and VI markets is a way to provide incentives. One part of the literature related to the market mechanism design of FR and VI focuses on the modeling of the frequency dynamics after a contingency and the formulation of the frequency nadir constraint in the security-constrained unit commitment (SCUC) and the security-constrained economic dispatch (SCED) problems. These two problems are parts of most clearing engines of the co-optimized energy and ancillary services market. The literature also discusses the way to price the FR and VI products. However, only a few works consider the dispatch process of the FR and VI products or allow the provider to bid a price for the FR or VI provision.

Therefore, in this project, we will propose a new bid structure for FR and VI which includes bid prices. Then, we will examine the patterns of dependencies among the price and amount of these two products. The results will help understand the features of the new market and probably inform further research on this type of market.

1.2. Research Question

The research question of this project is "**What are the patterns of dependencies in the frequency response (FR) and virtual inertia (VI) market with FR and VI prices as part of the bid?**"

- RQ1: how does the product frequency response (FR) sold relate to its price?
- RQ2: how does the size of the largest unit relate to the frequency response (FR) needed?
- RQ3: How does the virtual inertia (VI) relate to the price of virtual inertia (VI)?
- RQ4: How does the frequency response (FR) sold relate to the amount of virtual inertia (VI) sold?

[1] Contingency is defined in this as the loss of one conventional generator which causes the greatest frequency deviation. It is not necessary the largest unit online. It can, for example, the second largest unit with very large inertia constant

1.3. Outline of this Report

This report will be organized as follows. The chapter 2 will provide a review of related literature and basic theories in this project. After that, chapter 3 will describe the proposed bid structure and methodology for analysis in this project. The setup for the case study and the results will be shown in chapter 4. Finally, chapter 5 will summarize and conclude the report.

2

Literature and Basic Theories

The context of this research is to figure out the best way to procure ancillary services (AS) that contribute to frequency stabilization after the contingency of a generation outage. As essential parts of the clearing engine of the electricity market, the security-constrained unit commitment (SCUC) and security-constrained economic dispatch (SCED) decide the procurement of the AS, and the frequency constraints within these two algorithms embody the enforcement of the frequency-stability rules. The discussions in the literature mainly focus on the formulation of the frequency constraints, which are determined by the way of modeling the frequency dynamics of the power grid among other factors.

Therefore, this chapter will start with mathematical optimization, which is the fundamentals of the SCUC and the SCED. Then, the literature on modeling frequency dynamics and formulating frequency constraints is reviewed. After that, the formulation of SCUC and SCED in the most state-of-the-art literature is shown. Finally, we summarize the ways of settlement and payment in the electricity market in a stand-alone section.

2.1. Electricity Market and Its Clearing Engine

The electricity market minimizes the cost of power system operation and guarantees the security of electricity supply (SoS) in the short term. It consists of not only the energy market but also various AS markets as well. The SCUC and SCED are the main algorithms that clear the electricity market and decide the payment and settlement of the market. SCUC and SCED are a special type of UC and ED, which are all optimization problems.

Therefore, this section will start from the basics of mathematical optimization for the reference of the non-technical audience. Then, we will describe the general structure of the electricity market and the types of AS, especially the frequency services. After that, we will discuss the general formulation of the SCUC and SCED, which consider both energy and AS.

2.1.1. The Structure of the Electricity Market

The context of this project is in the electricity market. The energy market is the most important component of the electricity market to make sure that the demand for electricity and supply of electricity are balanced at any time.

The electricity market is categorized into two types: decentralized market and pool-based market. In a decentralized market, most of the energy transactions are in the form of bilateral contracts. The day-ahead market (DAM) and the real-time market (RTM) play a supplementary role. In a pool-based market, all energy provisions are bid (i.e., "pooled") into one day-ahead market (DAM) before clearing and pricing. In this type of market, a security-constrained unit commitment (SCUC) algorithm is used to clear the DAM, and a security-constrained economic dispatch (SCED) algorithm is used to clear the RTM. subsection 2.1.5 will describe these two algorithms in detail.

Bidding and Clearing in the Energy Market

In microeconomics, the market price is defined by the intersection point of the demand curve and supply curve, which corresponds to the point of market equilibrium in general. In an electricity market, the demand curve is a vertical line if the demand response (DR) is not considered, and the supply curve is a piece-wise step function as shown in Figure 2.1. The piece-wise step function is a merit order curve consisting of each generation unit. In this figure, the ochre bars represent nuclear power plants, the grey bars represent coal power plants, the purple bars represent gas power plants, and the blue bars represent hydropower plants.

The point where the demand curve meets the supply curve (market clearing point) defines the market clearing price π_{energy}. The equilibrium market price corresponds to the maximum social welfare, which is defined as the sum of consumer surplus (CS), as represented in Figure 2.1 by the white area to the left of the demand curve and above the price line, and provider surplus (PS), as represented by the white area below the price line and to the left of the merit order curve. Since the area to the left of the demand curve is fixed given a certain demand level and generation units, the point of maximum social welfare is equivalent to the point of minimum total accepted bid price, e.g., the sum of the product of energy bid (i.e., variable cost c^{var} of energy production) and accepted generation capacity, as represented by

$$\sum_{g \in G_{accepted}} c_g^{var} \cdot p_g$$

This value corresponds to the area below the merit order curve and to the left of the demand curve. Theoretically, in a fully competitive electricity market, the best way for a generation unit to bid in the market is to bid its marginal production cost, which is c^{var} for variable cost, in the unit of €/MWh, and c^{fix} for fixed cost c^{fix} in the unit of €$/h$. This is due to the rule of marginal pricing. If a generation unit is a marginal unit, it will set the market clearing price. However, if that unit bids a price higher than its variable cost, the entire bid is likely to be out of merit and get rejected, which means that it will miss any profit. If that unit bids a price lower than its variable cost, the bid will be sure to be admitted but will result in negative profit. Given that it is not known whether a generation unit will be a marginal unit before the market clears, it is the best strategy for generation units to bid their variable cost in the electricity energy market.

Figure 2.1 shows an example of the clearing result of the electricity energy market. Each vertical bar represents a generation unit. The width represents the active power and the height represents the energy bid price. The units to the left of the market clearing points are dispatched units, which are uniformly paid with the market clearing price π_{energy}. Therefore the total payment is

$$payment = \pi_{energy} \cdot \sum_{g \in G_{accepted}} p_g$$

Paying every generation unit with a uniform marginal price is called "pay-as-clear" in contrast to "pay-

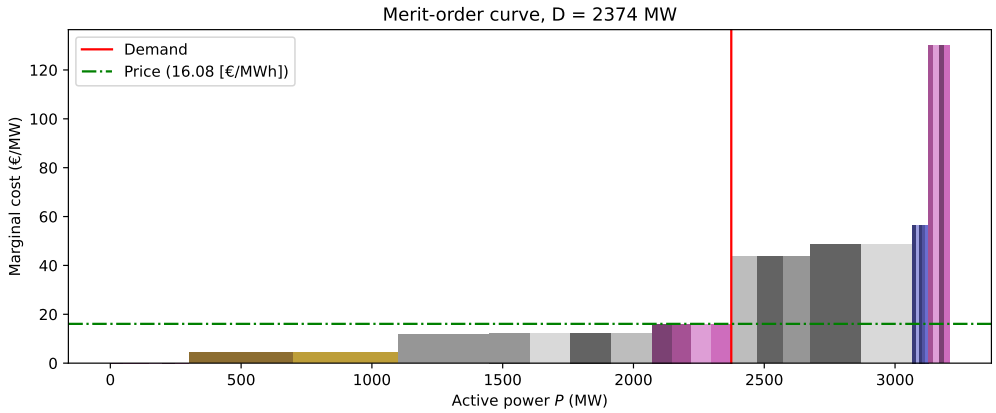

Figure 2.1: The merit-order curve in a classic economic dispatch (ED). All energy bids are ranked in ascending order based on their bid price. The top of the bars consists of the supply curve. The intersection point between the supply curve and the demand curve (the vertical line) represents the market equilibrium, or the market clearing point, which defines the market price at a market period. This result is the most cost-efficient way to supply the demand, hence the name "economic dispatch".

as-bid", where each generation unit is paid with its bid price c^{energy}.

2.1.2. Market Clearing Engine

The market clearing engine is usually an algorithm consisting of unit commitment (UC) or security-constrained unit commitment (SCUC) and economic dispatch (ED) and security-constrained economic dispatch (SCED). Therefore, in this subsection, we will introduce the general formulation of these problems.

2.1.3. Unit Commitment and Economic Dispatch

The market clearing result as shown in Figure 2.1 is calculated from the unit commitment (UC) or economic dispatch (ED) algorithm, which minimizes overall operational cost by considering a set of constraints. The objective function is the sum of the energy bid price

$$\sum_{g \in G_{accepted}} c_g^{energy} \cdot p_g$$

In classic UC and ED, the optimization is subjected to several physical and operational constraints [11], including the constraint for power balance, the upper and lower bound of the generation units as shown in Equation 2.1. Conventional power plants can only operate at an output level above the minimum stable generation (MSG), which defines the capacity lower bound ($\underline{P_g}$), and below their installed capacities, which defines the capacity upper bounds ($\overline{P_g}$). The difference between installed capacity and dispatched power defines the headroom capacity, i.e., $P_{hr} = \overline{P_g} - P_{t,g}$.

Some UC and ED algorithms also include the constraints for the speed limit of ramping up and down,

and the minimum time of turning on and off, which, for simplicity, are not considered in this project.

$$\min_{P_{t,g},y_{t,g}} \quad \sum_{t\in T,g\in G} y_{t,g}\cdot c^{fix} + \sum_{t\in T,g\in G} P_{t,g}\cdot c^{var} \tag{2.1a}$$

$$s.t. \quad \sum_{g\in G} P_{t,g} = d_t \qquad \text{(Power balance)} \tag{2.1b}$$

$$y_{t,g}\cdot \underline{P_g} \le P_{t,g} \le y_{t,g}\cdot \overline{P_g} \qquad \text{(Capacity limits)} \tag{2.1c}$$

$$\tag{2.1d}$$

Though there are the same set of decision variables and constraints in UC and ED, they are different from each other in multiple aspects. In UC, the decision variable for commitment status $y_{t,g}$ is a binary variable and thus the UC problems are usually mixed-integer linear programs (MILP). In ED, the commitment status is already known or the problem only considers committed units in the problem, and thus all decision variables in ED are continuous. Therefore, the ED problems are usually linear programs (LP), which have strong duality and provide dual values after solving the primal problem.

2.1.4. Ancillary Services Market and Co-optimization

The energy market guarantees the power balance at any time. However, the results from the classic UC and ED as shown in Equation 2.1 are not practical. Therefore, other requirements of system operation are included in the optimization problem. For example, the power flow along the transmission line should not exceed a certain level, the voltage at each node needs to be within a certain range, the post-contingency frequency dynamics should not violate a certain limit, the availability of reserve needs to be above a certain level in case that the generation or the load deviates from the scheduled level, so on and so forth.

To address these system security issues, the system operators also procure AS, such as secondary and tertiary frequency control, spinning and non-spinning reserve, reactive power injection, dispatch, and so on. In some markets, the ancillary services are procured in a market different than the energy market. In other markets, the ancillary services are cleared together with the energy market. The method that clears the energy and ancillary services market together is called “co-optimization”.

2.1.5. Security Constrained Unit Commitment and Economic Dispatch

In the co-optimized electricity market, the operational requirements of the system are included in the classic UC and ED algorithm as security constraints to decide the amount of ancillary service procurement, price them, and guarantee the security of system operation at the same time. In this case, the UC and ED upgrades to security-constrained unit commitment (SCUC) and security-constrained economic dispatch (SCED). The schedule of energy and ancillary services from the result of SCUC and SCED is then more practical in real operation.

While SCUC and SCED have the same set of constraints and the same set of decision variables, they have similar differences as the difference between classic UC and classic ED and are both used in the real electricity market, though in different scenarios. In pool-based electricity markets such as PJM and ERCOT, the day-ahead market (DAM) clears with the SCUC algorithm, and the real-time market (RTM) clears with the SCED algorithm. The SCUC decides the commitment status of generation units and active power dispatch preliminarily. Then, SCED inputs the unit commitment results decides the final result of active power dispatch after minor adjustment (based on RTM) and provides the dual values of each decision variable, which can be used to derive the pricing of energy and ancillary services.

Figure 2.2 visualizes the connection between SCUC and SCED.

The context of this project is SCUC and SCED with frequency stability constraints, which will be discussed in detail in section 2.2.

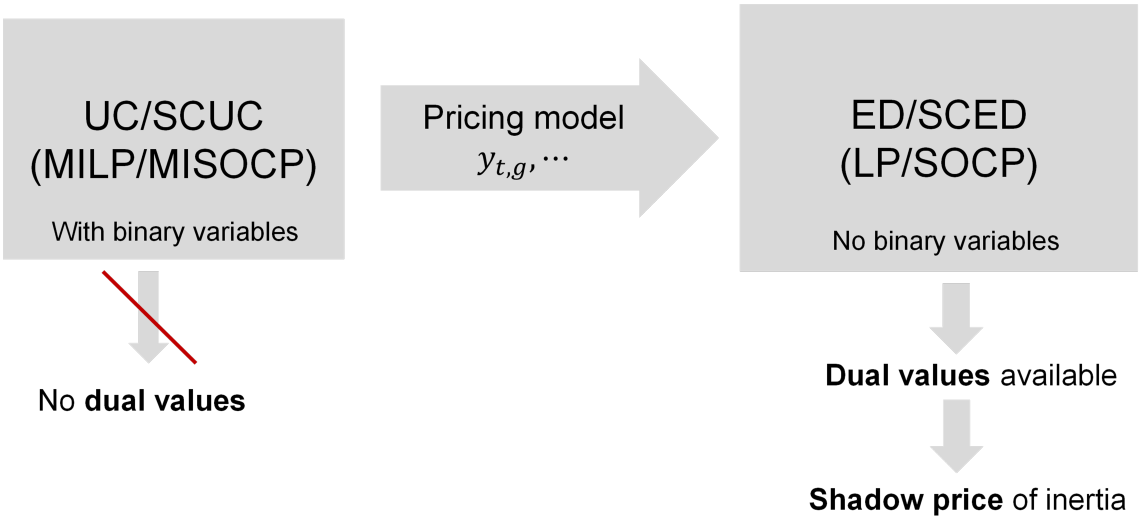

Figure 2.2: The connection between SCUC and SCED. SCUC decides the unit commitment of generation units and dispatches them preliminarily. Since there are binary variables, it is not possible to derive the dual values of constraints, and thus there is a barrier to pricing products. In contrast, there are no binary variables in the SCED problem. After assigning the results of binary variables in the SCUC problem to the corresponding variables in SCED, the SCED gets the same results as SCUC while keeping strong duality. Therefore, it is possible to derive the dual values of constraints from the optimization results, which can be used to price energy and ancillary services.

2.2. System Dynamics Modelling and Frequency Stability Constraints

Frequency stability after contingency is one of the system security requirements. A contingency is defined as the sudden loss of the largest generation unit (P^L). After a contingency, the system frequency will drop due to an imbalance between power supply and power demand and then be contained by frequency-responsive devices, as shown in Figure 2.3. However, some elements in the power system are vulnerable to frequency deviations. For example, the conventional generation units can only operate safely when the system frequency maintains above a certain level ($\omega \geq \underline{\Delta\omega}$). Therefore, there are under-frequency load sheddings (UFLS) in the system to protect these vulnerable units from under-frequency [12]. However, once UFLS happens, the system operator needs to compensate the energy users for the energy interruption. This introduces extra costs of system operation [11]. If UFLS fails to prevent system frequency from dropping, generation units start to disconnect from the system to protect themselves, enlarging the power imbalance and accelerating frequency drop, which may lead to a blackout. Besides frequency nadir limits, the rate of change of frequency (RoCoF) should also be within a reasonable range because some elements in the network are sensitive to the RoCoF. Moreover, after frequency responsive reserves, such as primary frequency response (PFR), are activated, the frequency needs to be stabilized at a certain level, which is above the frequency nadir limit ($\underline{\Delta\omega}$).

In summary, there are three typical frequency constraints, whose general formulations are

$$\omega'(k) \geq \underline{\omega'} \quad \forall k \in K \qquad \text{(RoCoF constraint)} \qquad (2.2a)$$

$$\omega(k \geq k_{qss}) \geq \underline{\Delta\omega_{qss}} \qquad \text{(QSS constraint)} \qquad (2.2b)$$

$$min(\omega(k)) \geq \underline{\Delta\omega} \quad \forall k \in K \qquad \text{(Nadir constraint)} \qquad (2.2c)$$

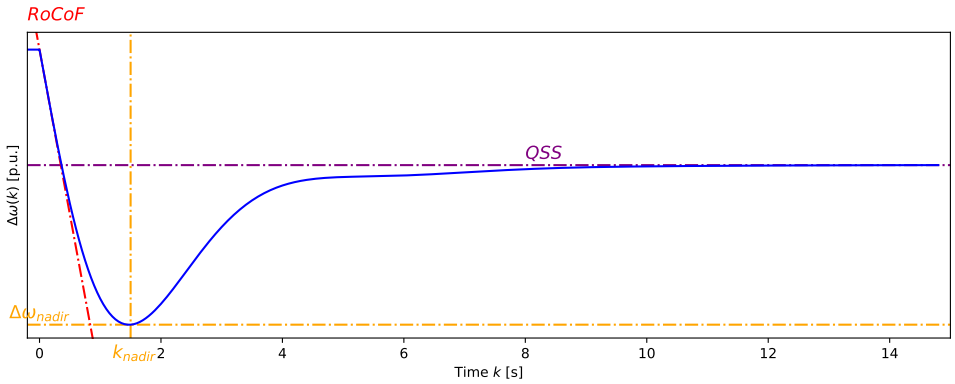

Figure 2.3: Frequency curve after contingency. The frequency drops at first due to power imbalance. After the activation of frequency-responsive services, the drop was decelerated until reaching a minimum frequency, which is the nadir frequency ($\underline{\Delta\omega}$). Then, the frequency starts to recover and finally stabilizes at a quasi-steady state (QSS) frequency, which is between the nadir frequency and the nominal frequency. The red dotted line represents the maximum rate of change of frequency (RoCoF) at $k = +0$ s. The horizontal purple line represents the quasi-steady state (QSS) frequency. The vertical and horizontal orange line represents the time of reaching the frequency nadir (k_{nadir}) and the nadir frequency ($\underline{\Delta\omega}$).

The specific formulation of these three constraints differs in the literature and depends on the way of modelling the frequency dynamics after contingency. The modelling used in the context of SCUC and SCED can be categorized into two types. The first type of system model is the **"full model"** [13, 11, 14, 6, 15], which models the behaviour of each element in the grid, such as load, hydropower plants, different types of thermal plants, in detail and then combines these models together into a system model. An example of a diagram representation of the **"full model"** can be found in [16]. The model is usually validated with historical operational data or simulation data and thus is accurate in describing the frequency dynamics after contingency. However, such a model is usually highly non-linear. Therefore, it is not possible to derive a closed-form expression of the frequency constraint from such a model or the formulation will be incompatible with the optimization problem. Another type of system model is the **"swing equation model"**, where the system frequency is modelled as a single equation, which will discussed in detail in the next subsection.

2.2.1. Swing Equation

The dynamics of synchronous machines are described by the swing equation (Equation 2.3) [17], which consists of the main behaviour of the system frequency. The acceleration rate of the steam or gas turbine (i.e., rotor) is proportional to the imbalance between the mechanical torque input T_m and the electromagnetic torque output to the electricity generator T_e. The coefficient of proportionality is decided by the momentum of inertia of the turbine J.

$$J\frac{d^2\delta}{dk^2} = T_m - T_e \tag{2.3}$$

where δ is the angular position of the rotor in rad, whose acceleration rate defines the angular velocity

$$\omega_m = \frac{d\delta}{dk} \tag{2.4}$$

and the power input and output is defined as

$$P_m = \omega_m \cdot T_m \tag{2.5}$$

$$P_e = \omega_m \cdot T_e \tag{2.6}$$

To be compatible with different sizes of synchronous machines, the inertia constant H in the unit of seconds is used in the coefficient of proportionality instead of the momentum of inertia of the rotor J. The inertia constant of a synchronous machine H_g equals the instantaneous kinetic energy of the rotor standardized by the size of the synchronous machine, i.e., the rated apparent power S_{rated}, as described in the following equation

$$H_g = \frac{1}{S_{rated}} \frac{J\omega_m^2}{2} \approx \frac{1}{\overline{P}} \frac{J\omega_{m,0}\omega_m}{2}. \tag{2.7}$$

The inertia constant at the rated angular velocity $\omega_{m,0}$ is a good approximation of the actual inertia constant in the power system operation. This is because to keep reliability, the power system maintains the system frequency $\omega(k)$ within a small range. Since the angular velocity of rotors $\omega_{m,0}$ is electromagnetically coupled with the system frequency $\omega(k)$, the error caused by the frequency deviation is small enough to be ignored. Moreover, in this project, the reactive power and voltage effects are not considered. The rated apparent power S_{rated} is approximated to be the capacity limit of the generation unit $\overline{P}$ (in MW).

Inserting Equation 2.7, Equation 2.5, and Equation 2.4 in to Equation 2.3, the swing equation becomes

$$\overline{P} \cdot \frac{2H_g}{\omega_{m,0}} \frac{\Delta\omega_m}{dk} = P_m - P_e = \Delta P_{rotor} \quad \forall g \in G \tag{2.8}$$

where inertia constant H_g is in the unit of seconds (s), angular velocity ω_m is in the unit of hertz (Hz) or rad/s, and the active powers are in the unit of megawatts (MW).

The angular velocity of each synchronous machine ω_g is electromagnetically coupled with the system frequency ω_{sys} (in Hz). In this project, they are considered identical and location effects are ignored

$$\omega_{m,g} = \omega_{sys}, \quad \forall g \in G \tag{2.9}$$

Inserting Equation 2.9 and summing up Equation 2.8 for all synchronous machines g in the system, i.e., G, the swing equation for the system frequency is written as

$$\sum_{g \in G} \overline{P}_g H_g \cdot \frac{2}{\omega_0} \frac{\Delta\omega_{sys}}{dk} = \Delta P_{sys} \tag{2.10}$$

Defining the per unit active power as

$$p = \frac{P}{P^{p.u.}} = \frac{P}{\sum\limits_{g \in G} P_g} \tag{2.11}$$

The active power in MW corresponding to per unit value is defined as the total generation capacity in

the system $\sum_{g \in G} P_g$. The per-unit system frequency is defined as

$$\omega = \frac{\omega_{sys}}{\omega_0} \tag{2.12}$$

The system-wide inertia constant H is then defined as the average of individual inertia constants H_g weighted by generation capacities $\overline{P}$

$$H = \frac{\sum_{g \in G} \overline{P} H_g}{\sum_{g \in G} P_g} = \frac{\sum_{g \in G} \overline{P} H_g}{P^{p.u.}} \tag{2.13}$$

Inserting Equation 2.11, Equation 2.12, and Equation 2.13 into Equation 2.8, the system-wise swing equation becomes

$$2H \cdot \frac{d\Delta\omega}{dk} = \Delta P(k) \tag{2.14}$$

where $\Delta P(k)$ is in per unit.

2.2.2. Solution of Swing Equation

The swing equation is hard to solve because it is an implicit differential equation, and $\Delta P(k)$ is usually highly non-linear and is dependent on frequency $\omega(k)$. However, if, after simplification, $\Delta P(k)$ is not dependent on frequency mathematically, the frequency dynamics $\omega(k)$ can be expressed as the integration of the swing equation, shown as follows

$$\omega(k) = \frac{1}{2H} \int_0^k \Delta P(k) dk + \omega(0) \tag{2.15}$$

$$\Delta\omega(k) = \frac{1}{2H} (\int_0^k -P^L + P_{other}(k)) dk \tag{2.16}$$

$$= \frac{1}{2H} (-P^L \cdot k + \int_0^k P_{other}(k) dk) \tag{2.17}$$

Therefore, whether the above expression is integrable depends on the dynamics of frequency-responsive devices, i.e., the formulation of $P_{other}(k)$.

2.2.3. System Models in the Context of Optimization Problem

In the context of SCUC and SCED, the details of the model is different in each literature. And the way that the model is incorporated into the algorithm is different. They are grouped into four general approaches, which will be discussed in this subsection.

External Constraints after Dynamic Simulation

In this approach, the "full model" is used to represent the system dynamics, as in the work by O'Sullivan et. al [18, 11], Ela et. al [6, 16], and Doherty et. al [14]. After the SCUC is run, the dispatch result is compared with an external frequency requirement (Equation 2.2). The optimization problem is run iteratively with different configurations, e.g., modified speed governor status [6], till all frequency requirements are fulfilled and the market is cleared for that market period. Figure 2.4 summarizes this approach.

There are limitations to this approach. For example, the system model is too detailed to solve in a short time. The iterative way of clearing the market also adds to the computational burden. As a result,

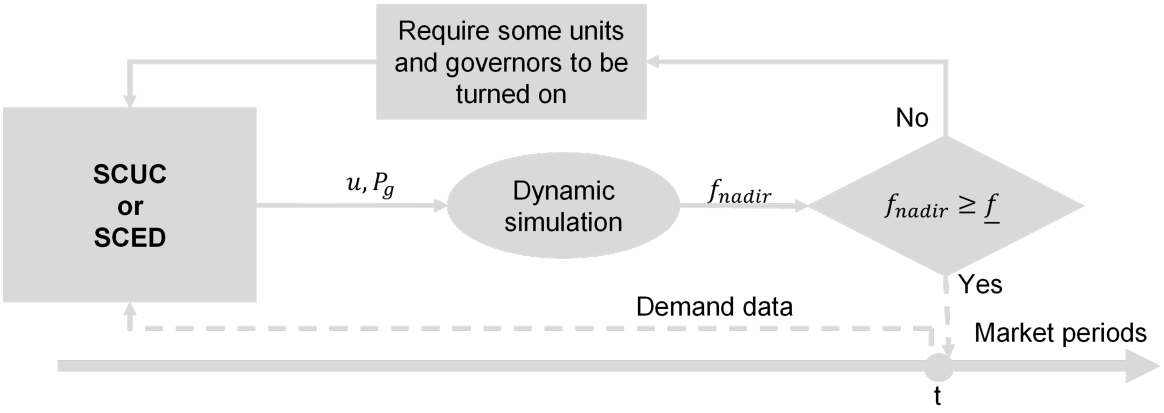

Figure 2.4: The **"external constraints after dynamic simulation"** approach to clearing the market. The dynamic simulation is external to the SCUC and SCED problems. The frequency requirements are not included in the optimization problem as constraints but are checked with the results of a system dynamics simulation after the SCUC or SCED. The optimization problem is run iteratively with slightly different configurations till all the frequency requirements are fulfilled. This approach is adopted in [13, 14, 6, 16, 5]

most of the algorithms in the literature based on this approach require a long time to solve, typically more than 15 minutes [16], which is not practical in most application scenarios. Moreover, the system model is complicated and not intuitive enough.

Internal Constraints with Fitted Dynamics

The system dynamics model is highly non-linear. Therefore, in this approach, the dynamics is fitted into simpler functions that are compatible with the optimization problem. Then, the frequency requirements can be included in the SCUC and SCED as constraints. In the literature, there are multiple different methods of fitting proposed. In the work by O'Sullivan et. al in 1996 [13], the system model is regressed into a Hessian matrix and gradients of the Lagrangian function as parameters of the SCED problem, which is a sequential quadratic program (SQP). In the work by Xu et. al in 2018 [19], the interdependence of virtual inertia provision and frequency nadir is piece-wise linearized and input into the optimization problem as parameters. In the work by Li et. al in 2020 [5], the interdependence of minimum requirement for inertia and minimum requirement for the primary frequency response (PFR) to fulfill the frequency nadir constraint is piece-wise linearized and input into the SCUC or SCED problem as parameters. Figure 2.5 summarizes the main procedures of this approach.

In this approach, a system dynamic simulation is also required for each market period though with a different aim than the previous approach. Compared to the **"external constraints after dynamic simulation"** approach, whose simulation results are used to check the frequency requirements, the simulation results in this approach are used to derive and update the parameters used in the frequency constraints, which are inside the SCUC and SCED algorithms. However, this approach has some limitations. The dynamic simulation needs to run multiple times with different parameter inputs to derive the results of simplification. The parameters in the SCUC and SCED need to be updated in each market period based on, e.g., load level and availability of renewables.

Numerical System Dynamics Inside Optimization Problem

In this approach, the way of modeling the system dynamics is fundamentally different from previous approaches.

Though the system dynamics is still described as non-linear implicit equations, some of which are differential equations, the number and complexity of those equations are reduced to the extent that

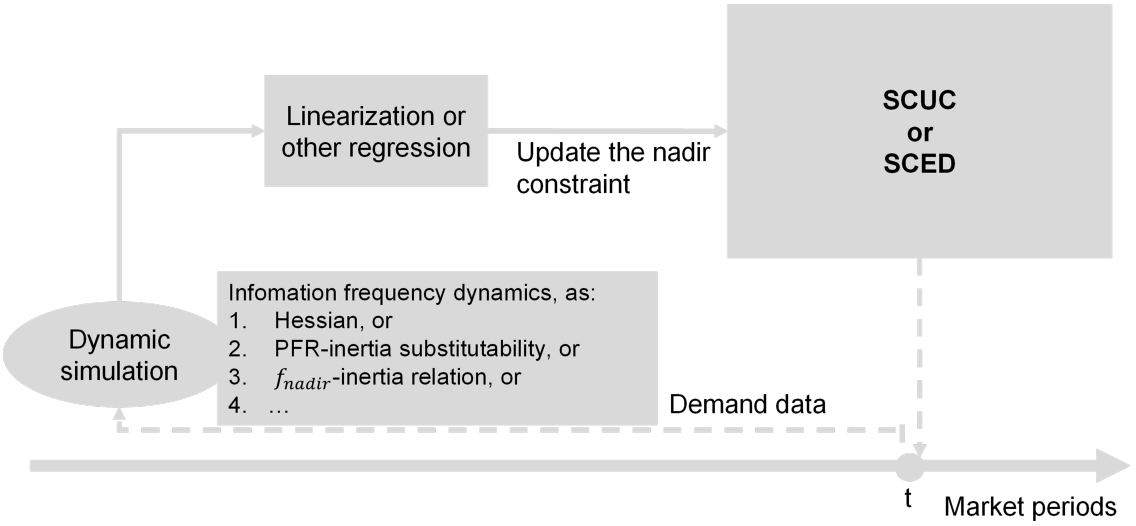

Figure 2.5: The **"internal constraints with fitted dynamics"** approach to clear the market. The system dynamic simulation is fitted into parameters, which are used to update parameters of the frequency constraints in the SCUC and SCED problems. The fitting can be piece-wise linearization (PWL), correlation between key variables, Hessian matrix, and so on. The SCUC or SCED only runs for one time per market period. This approach is used in [13, 19, 5, 15]

.

they can be included in the SCUC and SCED problems as equality constraints after discretization. The frequency dynamics $\Delta\omega(k)$, defined as a series of decision variables, is included in both inequality constraints for system dynamics and in the frequency constraints. After solving this optimization problem, both the generation schedule and the system dynamics are known.

Xu et. al [20] proposed this approach. Equation 2.18 shows the equality constraints used in [20] to model the system dynamic. The differential equations are transformed into discretized form in the algorithm. This system of equations models the behavior of the speed governor after a frequency trip in detail. Once the frequency deviation violates a certain threshold, i.e., frequency dead band $\Delta\omega_{db}$, the speed governor is activated, whose displacement gives a signal called "droop power order" $P_{g,t}^{c,r}$ [20], which aims to change the position of the steam or gas valve so that the mechanical torque on the turbine can be increased by sending more steam or hot air from the boiler or combustion chamber to the turbine. The "droop power order" is directly coupled with the frequency deviation $\Delta\omega(k)$ and is reversely proportional to the droop rate R_g^{droop}, which is described in Equation 2.18d.

The corresponding active power of the target valve position is described by the variable $P_{g,t}^{c,v}$. However, the valve reacts to the droop control with a delay, whose dynamics are described in Equation 2.18b. After the valve enlarges, there is another delay before the mechanical torque on the turbine increases to the target value that corresponds to the target of the valve position $P_{g,t}^{c,v}$, which is described by an intermediate variable representing the internal state of the lead-lag subsystem of the speed governor $P_{g,t}^{c,x}$. This delayed dynamics is described by the differential equation Equation 2.18c. The mechanical power output $P_{g,t}^{c,m}$ is a linear combination of both the valve position $P_{g,t}^{c,v}$ and the internal state of the lead-lag subsystem $P_{g,t}^{c,x}$, which is described in Equation 2.18e. The control loop is closed by the feedback from the active power to the frequency dynamics via the swing equation, i.e., Equation 2.18a.

In this approach, there is no iteration or fitting required. Besides, the dynamics of the speed governor are modeled in detail. However, there are limitations to this approach. The dynamics of other new elements, such as renewable generations, are not considered. The system of equations Equation 2.18

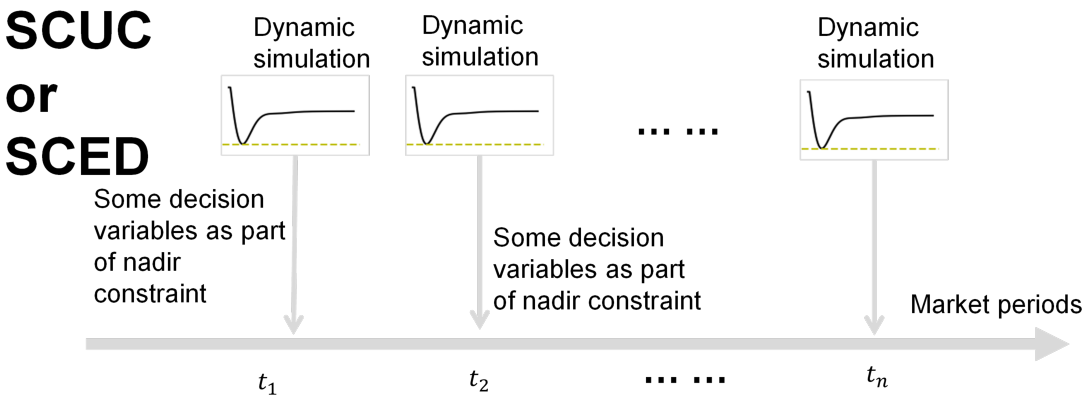

Figure 2.6: The **"internal system dynamics"** approach. The equations that model the system dynamics are discretized and included in the SCUC and SCED as equality constraints. The frequency dynamics $\Delta\omega(k)$, as a series of decision variables, is both in the equality constraints for the dynamics modeling and in the frequency constraints. After the algorithm is run, the system dynamics is also solved implicitly. This approach is used by [20].

increases the great computational burden on the algorithm due to the large number of decision variables and constraints. The maximum dimension of each decision variable is $T \times G \times K$, where T is the set of all market periods, G is the set of all generation units in the system, and K is the set of all time steps for the dynamic simulation. For example, a case study by us on the IEEE 24-bus reliability test system (RTS) for one single market period takes five minutes. It will take a much longer time for large systems and more market periods.

$$\sum 2H_g \frac{\Delta\omega_g(k)}{dk} = \sum P_{g,t}^{c,m}(k) - P^L - d_t - D\Delta\omega_t(k) \quad \text{(swing equation)} \tag{2.18a}$$

$$\frac{dP_{g,t}^{c,v}(k)}{dk} = \frac{1}{T_1}[P_{g,t}^{c,r}(k) - P_{g,t}^{c,v}(k)] \quad \text{(Delay of steam valve response)} \tag{2.18b}$$

$$\frac{dP_{g,t}^{c,x}(k)}{dk} = \frac{1}{T_3}[P_{g,t}^{c,v}(k) - P_{g,t}^{c,m}(k)] \quad \text{(Delay of an intermediate state)} \tag{2.18c}$$

$$P_{g,t}^{c,r}(k) = P_{g,0}^{c,m} - \frac{\Delta\omega(k)}{R_g^{droop}} \quad \text{(Droop order response to frequency)} \tag{2.18d}$$

$$P_{g,t}^{c,m}(k) = \frac{T_2}{T_3} P_{g,t}^{c,v}(k) + P_{g,t}^{c,x}(k) \quad \text{(Mechanical power output)} \tag{2.18e}$$

Analytical Dynamics Within Optimization Problem

Since the system dynamics is described by a system of differential and non-linear equations, as in the example of Equation 2.18, the frequency dynamics $\Delta\omega(t)$ is hard to solve in analytical form. Badesa et. al [21] proposed to simplify all types of frequency response as a linear ramp with different shapes, as shown in Figure 2.7, so that the swing equation is integrable.

The dynamics of active power injection from each individual frequency response device is

$$fr(k)\begin{cases} 0 & 0 \leq k \leq k^a \\ \overline{R} \cdot \frac{k-k^a}{k^b-k^a} & k^a \leq k \leq k^b \\ \overline{R} & k \geq k^b \end{cases} \tag{2.19}$$

Assuming that the damping effect of the load or other demand response is small enough to be ignored, and the only time-dependent active power injection is from the frequency response services, whose aggregate active power injection is $fr(k)$. Under these assumptions, the power imbalance term ΔP is equal to the sum of lost power P^L and the aggregate effect of frequency response, i.e., $fr(k)$ [21, 22, 23]. The swing equation becomes

$$2H \cdot \frac{d\Delta\omega(k)}{dk} = -P^L + fr(k) \tag{2.20}$$

whose integral is

$$\Delta\omega(k) = \frac{1}{2H}(-P^L \cdot k + \int_0^k fr(k)dk) \tag{2.21}$$

Since the linear ramp is easily integrable, the frequency dynamics $\Delta\omega(k)$ is solvable from Equation 2.21. Therefore, the minimum point k_{nadir} and the minimum value $\min(\Delta\omega(k)) = \Delta\omega(k_{nadir})$ is then possible to be derived from the frequency dynamics. This formula will also be adopted in this project.

Different from the models in all previous approaches, this model is not a precise description of the actual active power output from the frequency response service but only an underestimation. The frequency constraints derived from such modeling are therefore a conservative assumption, i.e., the constraints will fulfill the frequency requirement with a safety margin. Therefore, there will be an overestimation of the requirement for frequency response, which will compromise the economic efficiency to some extent.

However, there are multiple advantages provided by this proposal by Badesa et. al. [21, 22, 23]. Firstly, due to the integrability of the linear ramp, all three frequency constraints, especially the nadir constraint can be written in an analytical form. There is no dynamic simulation required in this algorithm, which makes the algorithm simple and easy to understand. Secondly, due to the analytical constraints, the SCUC and SCED have very low computational burden. It takes less than one second to run the algorithm in the case study of the simplified Great Britain network [23]. Thirdly, the linear ramp simplification applies to any type of frequency response services, not only conventional PFR but also FR from inverter-based resources (IBR). Therefore, this way of modeling is compatible with frequency response products with different dynamics and can be applied to potential new products. In short, the linear ramp provides a standard template for different FR providers to bid into the market. Finally, the dynamics are described in a simple way. Only three parameters are required to define a linear ramp, which is the time delay of FR activation k^a, time of full delivery k^b, and the FR capacity after full activation $\overline{R}$.

Nevertheless, the formulation proposed by Badesa et. al in their series of works [21, 22, 23] has limitations. While theoretically, the analytical nadir constraints apply to the market with any number of different FR products, the series of works only provide the formulation for the case of two different products, which are PFR provided by conventional speed governors, and enhanced frequency response (EFR) provided by renewable IBR. Moreover, the formulation in their works only considered the scenario that EFR starts to activate after the full activation of PFR, i.e., $k^a_{EFR} \geq k^b_{PFR}$. However, different

FR providers may have fundamentally different dynamics (k^a, k^b, and $\overline{R}$) and it is highly probable that there is overlapping time in the activation process of different products. If all these products, whose linear ramps are defined by customized parameters, are considered in the ancillary services market, the mathematical process of deriving the analytical nadir constraints will be too complicated to be practical, especially considering the fact that the mathematical derivation process is usually only possible to be done manually rather than automatically with computers.

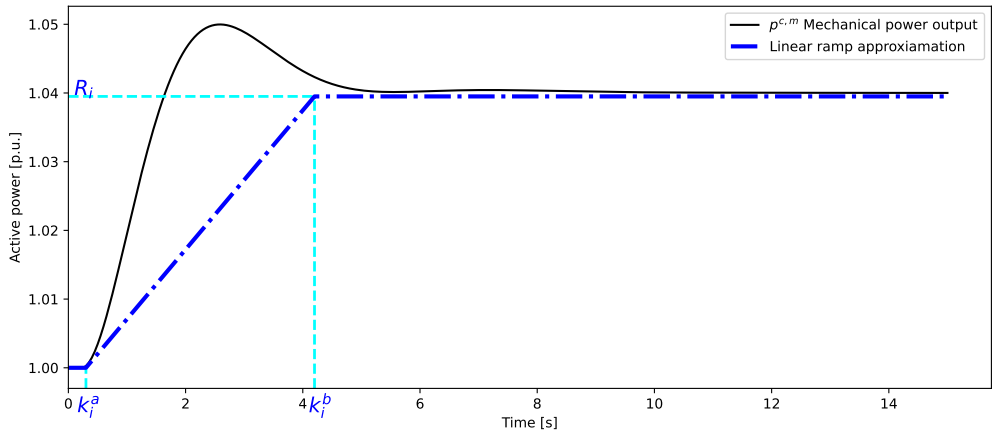

Figure 2.7: Activation dynamics of primary frequency response and its approximation as a linear ramp. The approximated curve is always below the actual power output. Therefore, the resulting frequency dynamics is a conservative assumption. This linear-ramp simplification can be applied to all types of frequency response in the context of the ancillary services market. [21, 22, 23]

2.2.4. Constraint for the Rate of Change of Frequency

The rate of change of frequency (RoCoF) is defined as the first derivative of the frequency dynamics $\omega(k)$, i.e., $RoCoF = \omega' = \Delta\omega'$, which is visualized as the oblique red line in Figure 2.3. After choosing the way of modeling the system dynamics, the detailed formulation of those three frequency stability constraints (Equation 2.2) can be decided. The rate of change of frequency (RoCoF) constraint is nearly the same in all literature because the maximum absolute RoCoF usually does not depend on the dynamics but rather occurs immediately after the beginning of a contingency (i.e., when $k = +0$ s) because the power imbalance reaches its largest value at that moment, i.e., $\Delta P(k = +0\ s) = -P^L$. Therefore, the RoCoF constraint can be formulated as

$$-\frac{P^L}{2H} \geq \underline{\omega'} \tag{2.22}$$

where $\underline{\omega'}$ is the RoCoF limit and is a negative value.

2.2.5. Quasi-Steady State Constraint

After the contingency, frequency-responsive devices increase their power injection into the network to compensate for the power imbalance. After several seconds, the frequency deviation is contained and reaches a quasi-steady state (QSS) level at a frequency between the frequency nadir requirement and the lower bound of the normal operation, which is within the deadband of speed governors. The QSS frequency is visualized as the horizontal purple line in Figure 2.3.

There are generally two ways to formulate the QSS constraint. Equation 2.2b makes sure that the

QSS frequency is above a certain requirement. This requires that the frequency curve is solved, and thus this formulation is applicable to approaches of algorithms discussed in subsection 2.2.3. However, in the work by Badesa et. al [21, 22, 23], the QSS constraint is not included. Instead, the authors made sure that there is sufficient capacity for frequency response to compensate for the power imbalance due to the contingency after the full activation, i.e.,

$$\sum_{i \in I} fr(k) \geq P^L \tag{2.23}$$

2.2.6. Nadir Constraint

In the first approach discussed in subsection 2.2.3, i.e., **"External Constraints after Dynamic Simulation"**, there is no nadir constraint within the optimization problem. Equation 2.2c is checked with the results of the system dynamic simulation after the SCUC or SCED.

$$min(\omega(k)) \geq \underline{\Delta\omega}, \qquad \forall k \in K$$

In the second approach, i.e., **"Internal Constraints with Fitted Dynamics"**, the nadir constraint takes the same format as the equation above, but (1) it will be an inequality constraint in the SCUC or SCED problem, and (2) the term $min(\omega(k))$ is an expression with decision variables and fitted parameters from the system dynamic model.

In the third approach, i.e., **"Numerical System Dynamics inside Optimization Problem"**, the nadir frequency or the time of reaching the nadir is not known before the optimization problem is solved. Therefore, the decision variable representing frequency deviation $\Delta\omega[k]$ is constrained by the nadir requirement at all simulation time steps ($\forall k \in K$). The frequency nadir constraint is formulated as follows [20].

$$\Delta\omega[k] \geq \underline{\Delta\omega} \quad \forall k \in K \tag{2.24}$$

In the last approach, i.e., **"Analytical Dynamics within Optimization Problem"**, the frequency nadir constraint is written as a second-order cone (SOC) of decision variables, including available inertia H, available FR capacity from each provider R_i, and the largest online unit or the size of the largest unit P^L.

2.3. Frequency-Constrained SCUC and SCED

In the work by Badesa et. al [21, 22, 23], the SCUC, and SCED are formulated as follows.

Objective function:

$$\min_{P_{t,g}, y_{t,g}} \quad C^{fix} + C^{var} + C^{FR} \tag{2.25a}$$

$$= \sum_{t \in T, g \in G} y_{t,g} \cdot c^{fix} + P_{t,g} \cdot c^{var} + \sum_{i \in I} x_i \cdot R_i \cdot c_i^{FR} \tag{2.25b}$$

Constraints in classic UC and ED:

$$s.t. \quad \sum_{g \in G} P_{t,g} = d_t \qquad \forall t \in T \quad \text{(Power balance)} \tag{2.25c}$$

$$y_{t,g} \cdot \underline{P_g} \leq P_{t,g} \leq y_{t,g} \cdot \overline{P_g} \qquad \forall g \in G, \forall t \in T \quad \text{(Capacity limits)} \tag{2.25d}$$

Defining the size of the largest unit:

$$P_t^L \geq P_{t,g} \qquad \forall g \in G, \forall t \in T \quad \text{(size of the largest unit)} \tag{2.25e}$$

Frequency constraints:

$$\sum_{i \in I} R_{t,i} \geq P_t^L \qquad \forall t \in T \quad \text{(re-balancing constraint)} \tag{2.25f}$$

$$-P_t^L \geq 2H_t \cdot \omega'_{min} \qquad \forall t \in T \quad \text{(RoCoF constraint)} \tag{2.25g}$$

$$\left\| \begin{bmatrix} \frac{1}{f_0} & -\frac{k_1^a + k_1^b}{4\Delta f_{max}} & \frac{{k_2^a}^2}{k_2^b \cdot 4\Delta f_{max}} - \frac{1}{k_2^b} & 0 \\ 0 & -\frac{1}{\sqrt{\Delta f_{max}}} & \frac{k_2^b}{k_2^b \sqrt{4\Delta f_{max}}} - \frac{1}{k_2^b} & \frac{1}{\sqrt{\Delta f_{max}}} \end{bmatrix} \begin{bmatrix} H \\ R_1 \\ R_2 \\ P^L \end{bmatrix} \right\|$$

$$\leq \begin{bmatrix} \frac{1}{f_0} & -\frac{k_1^a + k_1^b}{4\Delta f_{max}} & \frac{{k_2^b}^2}{k_2^b \cdot 4\Delta f_{max}} + \frac{1}{k_2^b} & 0 \end{bmatrix} \begin{bmatrix} H \\ R_1 \\ R_2 \\ P^L \end{bmatrix} \qquad \forall k \in K, \forall t \in T \quad \text{(Nadir constraint)} \tag{2.25h}$$

In this project, we will build our methodology on this formulation for the SCUC and SCED problem. We will add a QSS constraint and develop a different formulation of the frequency nadir constraint.

2.4. Pricing and Payment

In this project, both the energy market and the frequency response markets are considered. These products are priced after the SCUC and SCED algorithms are run. In this section, we will discuss the method of pricing energy and frequency response in the works by Badesa et. al [21, 22, 23].

2.4.1. Pricing of Energy

In the context of classic unit commitment (UC) and economic dispatch (ED), the only product in the market is energy. Its clearing price is set by the variable cost of the marginal unit, which is also the most expensive unit online.

2.4.2. Pricing of Frequency Response

In the works by Badesa et. al [22, 23], the authors assigned shadow prices to frequency services, including inertia, reduced the size of the largest unit, and frequency response. The formulas are shown

below

$$\pi_H = \frac{\mu - \lambda_1}{f_0} + 2\lambda_R \tag{2.26}$$

$$\pi_{P^L} = -\frac{\lambda_2}{\sqrt{\Delta f_{max}}} - \frac{\lambda_R \cdot f_0}{|\underline{\omega'}|} - \lambda_{qss} \tag{2.27}$$

$$\pi_R = \frac{\lambda_2}{\sqrt{\Delta f_{max}}} - (\mu - \lambda_1)\frac{k_1^a + k_1^b}{4\Delta f_{max}} + \lambda_{re-balance} \tag{2.28}$$

where μ, λ_1, and λ_2 are the dual values of the nadir constraint (a SOC formula), λ_R is the dual value of the RoCoF constraint, $\lambda_{re-balance}$ is the dual value of the re-balancing constraint, f_0 is the nominal frequency, Δf_{max} is the absolute value of frequency deviation at nadir, k_1^a is the activation delay of the first FR product, k_1^b is the delivery speed of the first FR product, and $|\underline{\omega'}|$ is the absolute value of the RoCoF limit.

2.4.3. Pricing Model

As mentioned in subsection 2.1.3 and subsection 2.1.5 and visualized in Figure 2.2, there should be a connection between the UC and ED algorithm or between the SCUC and SCED algorithm. This is because there are dual variables available in ED or SCED but not in UC or SCUC due to the existence of binary variables. However, the UC or SCUC is still required in order to get the commitment status, which is input to the ED or SCED algorithm.

In general, there are three methods of connecting SCUC and SCED, which is named as "pricing model" in the works by Badesa et. al [22, 23, 24, 25], there are three methods of connection mentioned, which are

- Dispatchable model. The binary variables, such as the unit commitment status y, are directly relaxed from a binary variable to a continuous variable bounded between 0 and 1, i.e., from $y \in \{0, 1\}$ to $y \in [0, 1]$. However, while there will be dual values available, the results may be practical in real operation because a unit can only be turned on or turned off. There is no intermediate status. Therefore, when y is not equal to 0 or 1, the SCED result will no longer be practical. This pricing model is used in most of the previous literature [23].
- Restricted model. The solution of y in the SCUC algorithm will be directly assigned to the y in SCED, i.e., there will be extra constraints in the SCED algorithm

  $$y_{t,g} = y_{t,g}^{scuc,\star} \tag{2.29}$$

  where $y_{t,g}^{scuc,\star}$ is the solution of y in the SCUC problem.
- Convex hull model. As mentioned in [22], this method minimizes the make-whole payment but introduces a large computational burden.

In this project, we will adopt the restricted model as the connection between the SCUC and the SCED problem. The details will be described in the next chapter.

3

Methodology

As mentioned in Section 2.2.3, the works by Badesa et. al [21, 22, 23] proposed a useful mathematical framework to model all types of frequency response (FR) services as linear ramps (Figure 2.7), formulate the nadir constraint in analytical form, and price them with shadow prices. However, in practical scenarios, there are some limitations, as mentioned in Section 2.2.3. When the number of FR products is more than two and the number is not known beforehand, the formulation of the analytical nadir constraint needs to be derived manually, which is time-consuming and not likely to be carried out with algorithms. This means that the method is not yet directly applicable to the actual scenario.

Moreover, the modeling focuses on the dynamics of known FR. The methodology used in this project will also consider the bidding and dispatch process of FR products. The FR bids can be either accepted or rejected. For example, if there is some available FR provided by an IBR with an amount of $\overline{R}$, it is desirable that the FR market only accepts part of the capacity, which is $R < \overline{R}$ if accepting the whole bid ($\overline{R}$) will result in over-supply of FR.

Therefore, in this project, numerical formulation of nadir constraint is adopted. A series of binary decision variables $x[t, i]$ are introduced to denote whether each FR bid is accepted. Moreover, The decision variable for accepted FR capacity R is introduced to distinguish from available FR capacity $\overline{R}$. Each of these new points in the approach of this project will be discussed in this chapter.

3.1. Bid structure

The main design of the FR and VI market can be summarized by the bid structure. In the FR market, each bid consists of five parameters, which are the time delay of activation k^a, the activation speed k^b, the available FR capacity $\overline{R}$, the bid price per megawatt capacity c^{fr}, and a binary parameter to indicate whether the bid is flexible. An example bid is shown in Table 3.1. If the “Flexible?” parameter is selected to be “True”, the bid can be partially accepted, which means that $R \in [0, \overline{R}]$ is possible. Otherwise, the bid can only be fully accepted or rejected, i.e., $R \in \{0, \overline{R}\}$. The former case is a description of the FR from IBR, whose control algorithm can adjust to different amounts of FR capacity. If the “Flexible?” parameter is selected to be “False”, the bid can only be completely accepted or rejected, which means that $R = x \cdot \overline{R}$, where x is a binary decision variable indicating whether the bid is accepted ($x = 1$) or rejected ($x = 0$). The inflexible bid is a description of a conventional FR provider, such as PFR from speed governors. The activation dynamics of PFR only depend on the dynamics of frequency

deviation $fr^{PFR}(k) = f(\Delta\omega(k))$ and the droop setting, which can not be provided partially. In this case, the binary decision variable x plays the same role as the binary variable to indicate whether the speed governor is enabled or not in the series of works by Ela et. al [6, 16]. There are an infinite number of FR products because each pair of k^a and k^b defines a different FR product if different quality.

Table 3.1: Example of FR bids in each market period. There is an infinite number of possible FR products, each defined by different pairs of time delay k^a and delivery speed k^b. A FR bid is defined by five parameters. Other parameters are the capacity, or amount, of FR (R), the price of FR (c^{fr}), and a boolean value indicating whether the FR bid is flexible or not. If the bid is flexible, the dispatched FR capacity can be any value equal to or below the bid amount, i.e., $R \in [0, \overline{R}]$; if the bid is inflexible, the dispatched FR capacity can only be zero (rejected) or the full bid amount (fully accepted), i.e., $R \in \{0, \overline{R}\}$

Market period t	Provider i	k^a	k^b	$\overline{R}$	c^{fr}	Flexible?
1	Wind 1	3 s	8 s	10 MW	12 €/MW·h	True
1	Gas 2	0 s	5 s	30 MW	15 €/MW·h	False
2	Wind 1	2 s	4 s	15 MW	12 €/MW·h	True
2	Gas 2	0 s	5 s	30 MW	15 €/MW·h	False
2	Solar 1	0 s	5 s	15 MW	12 €/MW·h	True
3	Coal 1	3 s	6 s	50 MW	8 €/MW·h	False
...	...	...	...	...	...	...

The VI bids only has three parameters, which are the amount of bid ($\overline{H_{vi}}$), the price of bid (c^{fr}), and a boolean value to indicate whether the bid is flexible or not. Unlike FR products, there is only one type of VI product.

Table 3.2: Example VI bids in each market period. There is only one type of VI product. Therefore, there are three parameters in each VI bid, which are the amount of VI ($\overline{H_{vi}}$), the price of VI (c^H), and a boolean value indicating whether the VI bid is flexible or not. If the VI bid is flexible, the dispatched VI amount can be any value equal to or below the bid amount, i.e., $H_{vi} \in [0, \overline{H_{vi}}]$; if the VI bid is inflexible, the dispatched VI amount is either zero (rejected) or equal to the full amount (fully accepted), i.e., $H_{vi} \in \{0, \overline{H_{vi}}\}$

Market period t	Provider j	$\overline{H_{vi}}$	c^H	Flexible?
1	Wind 2	1000 MW-s	1.05 €/MW-s	True
1	Solar 2	2000 MW-s	0.8 €/MW-s	True
2	Wind 2	900 MW-s	1 €/MW-s	True
2	Solar 2	2100 MW-s	0.8 €/MW-s	True
2	Solar 3	1100 MW-s	0.65 €/MW-s	True
3	Wind 2	1000 MW-s	1.1 €/MW-s	True
...	...	...	...	...

3.1.1. Per Unit System

For simplicity and generalization, we formulate the SCUC and SCED problems in per unit system. Table 3.3 gives some examples of translating original values to per-unit values. The general rules of per unit system are as follows: for values related to active power, including dispatched power ($P_{g,t}$),

FR capacity ($R_{t,i}$), the size of the largest unit (P^L), costs (c^{var}, c^{fix}, c^{fr}, and c^H), inertia and virtual inertia (H), the conversion coefficient is the per unit active power ($P^{p.u.}$), which is selected as the total installed generation capacity (P^{tot}). For values related to frequency, including frequency nadir ($\Delta\omega_{min}$), RoCoF (ω'), QSS frequency ($\Delta\omega_{qss}$), the conversion coefficient is the nominal frequency (f_0), which is selected as 50 Hz in this project. It is worthwhile to mention that the inertia constant of the entire grid (in the unit of seconds) is already a per-unit value. The virtual inertia in megawatt-seconds, when converted to per unit value in seconds, can be directly added to the original system inertia constant (H) and becomes the aggregated inertia constant of the system ($H+H_{vi}$). In the next section, all equations and expressions are formulated in a per-unit system.

Table 3.3: Examples of conversion to per unit values.

Variable	Original value	Conversion coefficient	Per unit value
Active Power	400 MW	$P^{p.u.} = 25.664$ GW	$P_{t,g} = 0.0156$
FR capacity	32.08 MW	$P^{p.u.} = 25.664$ GW	$R_{t,i} = 0.00125$
Virtual Inertia	3208 MW· s	$P^{p.u.} = 25.664$ GW	$H_{vi} = 0.125\ s$
Fuel Cost	1 €/MWh	$P^{p.u.} = 25.664$ GW	$c^{var} = 25{,}664$ €$/p.u.\text{-}h$
Nadir Frequency	0.25 Hz	$\omega^{p.u.} = 50\ Hz$	$\Delta\omega_{min} = 0.005$
RoCoF	1 Hz/s	$\omega^{p.u.} = 50\ Hz$	$\omega' = 0.02/s$

3.2. The Frequency Constraints

Since the RoCoF constraint is not related to the FR dynamics, the formulation is the same as in most articles in the literature, which is

$$-P^L \geq 2H \cdot \Delta\omega'_{min}, \tag{3.1}$$

where p^L is the active power of the largest dispatched unit (abbreviated as “the size of the largest unit” in the following text). Total inertia H consists of both virtual inertia (H_{vi}) and physical inertia (H_{phy}). And $\underline{\Delta\omega'}$ is the RoCoF limit.

The frequency nadir constraint and the quasi-steady state (QSS) constraint are related to the FR dynamics. In this project, they are formulated based on the discrete FR dynamics and are named “numerical constraints” for convenience. They are included in the SCUC and SCED algorithms. The analytical nadir and QSS constraints, when there is a single type of FR dynamics, will also be formulated. The analytical constraints will only be used to help explain the results based on the numerical constraints.

Different from the analytical formulation, the expressions for the time of reaching frequency nadir k_{nadir} and the nadir frequency $min(\Delta\omega)$ are not known before solving the SCUC and SCED algorithm. Therefore, the activation dynamics of FR and its integral need to be discretized on time dimension (K). After discretization and integration, the instantaneous frequency deviation $\Delta\omega(k)$ is written as a linear expression of R. Finally, the expression for frequency deviation $\Delta\omega(k)$ is constrained by the frequency nadir limit $\underline{\Delta\omega_{min}}$ at each time step k

$$\Delta\omega(k) \geq \underline{\Delta\omega_{min}}, \qquad \forall k \in K \tag{3.2}$$

where K is the set of all-time steps k in the dynamic simulation. The key is to derive the expression of $\Delta\omega(k)$. To begin with, the following subsection will reformulate the swing equation.

3.2.1. Integral of FR Dynamics

As shown in Equation 2.21, one of the terms in the expression of $\Delta\omega(k)$ is the integral of fr on the time scale.

As formulated in Equation 2.19, the activation dynamics of each frequency response (Figure 2.7) is

$$fr(k^a, k^b, R, k) = \begin{cases} 0 & 0 \leq k \leq k^a \\ R \cdot \frac{k-k^a}{k^b-k^a} & k^a < k < k^b \\ R & k \geq k^b \end{cases} \tag{3.3}$$

The $FR(k)$ curve is integrated as follows

$$\int_0^k fr(k^a, k^b, R, k) = \begin{cases} 0 & 0 \leq k \leq k^a \\ R \cdot \frac{(k-k^a)^2}{2(k^b-k^a)} & k^a < k < k^b \\ R \cdot [\frac{k^b-k^a}{2} + (k-k^b)] & k \geq k^b \end{cases} \tag{3.4}$$

We introduce a function FR, which is the integral of $fr(k)$ when $R = 1$ (unitless),

$$FR(k^a, k^b, k) = \begin{cases} 0 & 0 \leq k \leq k^a \\ \frac{(k-k^a)^2}{2(k^b-k^a)} & k^a < k < k^b \\ \frac{k^b-k^a}{2} + (k-k^b) & k \geq k^b \end{cases} \tag{3.5}$$

which only depends on the delay k^a and delivery time k^b. Then, the integral of $FR(k)$ can be written as

$$\int_0^k fr(k^a, k^b, R, k) = R \cdot FR(k^a, k^b, k) \tag{3.6}$$

where R is a series of decision variables and all other inputs are parameters. While the function FR itself is non-linear, it will not influence the linearity of the SCUC and SCED problem because the output of FR is a constant. Thus the term FR is proportional to the decision variable R.

3.2.2. Discretization of FR Dynamics

Since the analytical formulation of the nadir constraint is not practical in the case of an unknown number of FR products, the activation dynamics of each FR product are discretized so that they can add up at each time step.

The relevant time range for the simulation is selected as $0 \leq k \leq K_s$, where K_s is selected as 10 s. The resolution of the time step is selected as $dk = 0.05$ s. Therefore, the set of time steps is

$$K = \{0, dk, 2dk, .., K_s\} = \{0, 0.05, 0.1, ..., 10\}\ s \tag{3.7}$$

After inserting each element k of the set K, the function $FR(k^a, k^b, k)$ becomes a time series

$$FR = \{FR[k] \mid \forall k \in K\} \tag{3.8}$$

3.2.3. Formulation of Numerical Nadir Constraints

Inserting the set of discretized and integrated FR activation dynamics FR (Equation 3.8) into the integrated swing equation (Equation 2.21), the frequency dynamics is

$$\Delta\omega[k] = \frac{1}{2H}(-P^L \cdot k + R \cdot FR[k]) \tag{3.9}$$

Therefore, the frequency nadir constraint will become

$$-P^L \cdot k + \sum R \cdot FR[k] \geq 2H \cdot \underline{\Delta\omega_{min}} \quad \forall k \in K \tag{3.10}$$

where P^L and R are decision variables, k is the iterator on the set K, H is the total inertia at the moment (including both physical inertia and virtual inertia), and $FR[k]$ and $\underline{\Delta\omega_{min}}$ are parameters. This is a linear constraint.

3.2.4. Formulation of QSS Constraints

The QSS constraint in the works by Badesa et. al [21, 22, 23] makes sure that there are enough FR to compensate for the active power loss due to contingency

$$\sum R \geq p^L \tag{3.11}$$

In this project, we will use the name “re-balancing” for this constraint and add another QSS constraint that requires the frequency to be contained above $\underline{\Delta\omega_{qss}}$ within time Ks. Therefore, the general formulation is as follows

$$\Delta\omega_{qss}(Ks) \geq \underline{\Delta\omega_{qss}} \tag{3.12}$$

The FR is fully activated at time Ks. Therefore, $FR[Ks] = 1$. Insert the expression of frequency deviation (Equation 3.9) into Equation 3.12, the QSS constraint is

$$-P^L \cdot Ks + \sum R \geq 2H \cdot \underline{\Delta\omega_{qss}} \quad \forall k \in K \tag{3.13}$$

3.2.5. Analytical Nadir Constraint for Single FR Dynamics

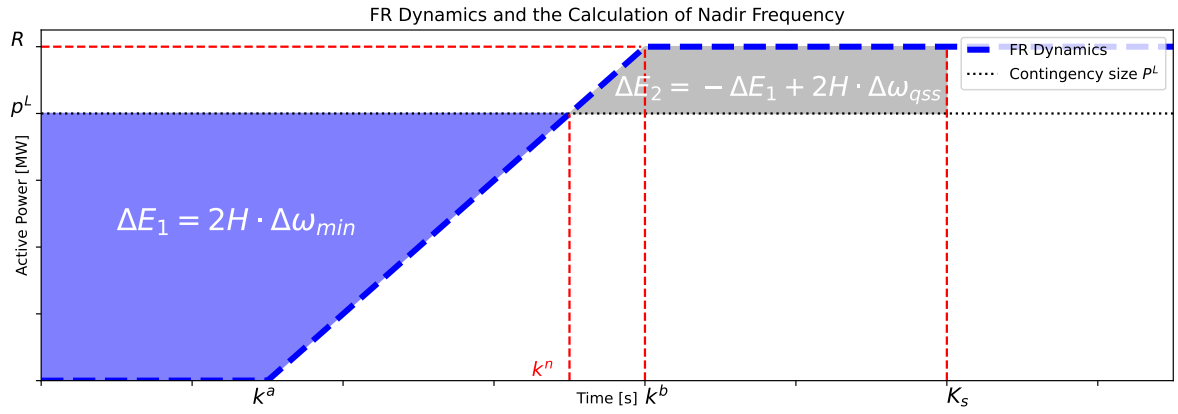

Figure 3.1: Dynamics of a Single FR Product and the Graphic Expression of the Nadir Frequency. The shadow area is the accumulated energy mismatch (ΔE) till the time of frequency nadir k^n. The nadir frequency can be calculated from it.

The blue area in Equation 3.3 gives the dynamics of a single standard FR. The frequency nadir happens during the activation of FR, i.e., $k^a \leq k^n \leq k^b$. Therefore, at frequency nadir

$$R \cdot \frac{k^n - k^a}{k^b - k^a} = p^L \tag{3.14}$$

$\therefore$ The time of frequency nadir is

$$k^n = k^a + (k^b - k^a)\frac{p^L}{R} \tag{3.15}$$

Figure 3.1 shows the geometric representation of the accumulated energy mismatch (ΔE). The nadir frequency can be derived as follows

$$\begin{aligned}
\Delta\omega(k^n) &= -\frac{1}{2H}\Delta E && (3.16)\\
&= -\frac{1}{2H}\frac{(k^a + k^n)p^L}{2} && (3.17)\\
&= -\frac{1}{4H} \cdot p^L[k^a + k^a + (k^b - k^a)\frac{p^L}{R}] && (3.18)\\
&= -\frac{1}{4RH} \cdot [2k^a R \cdot p^L + (k^b - k^a){p^L}^2] && (3.19)\\
&\geq \underline{\Delta\omega} && (3.20)
\end{aligned}$$

Therefore, the frequency nadir constraint is

$$-[2k^a R \cdot p^L + (k^b - k^a){p^L}^2] \geq 2RH\underline{\Delta\omega} \tag{3.21}$$

When total inertia H is constant, the nadir constraint can be solved as

$$p^L = \frac{\sqrt{k^a \cdot R^2 - 4(k^b - k^a)\underline{\Delta\omega}H \cdot R} - k^a \cdot R}{k^b - k^a} \tag{3.22}$$

3.2.6. Analytical QSS Constraints for Single FR Dynamics

The sum of the blue and the grey area in Figure 3.1 gives the accumulated energy imbalance till the time of quasi-steady state (Ks). Since at quasi-steady state, the FR is fully activated, i.e., $fr(Ks) = 1$, the frequency deviation is as follows

$$\Delta\omega(K_s) = \frac{1}{2H}(-K_s^a p^L + R) \tag{3.23}$$

$$= \frac{1}{4H}[-2K_s p^L + (2K_s - k^b - k^a)R] \tag{3.24}$$

$$\geq \underline{\Delta\omega_{qss}} \tag{3.25}$$

Therefore, the QSS constraint is formulated as

$$-2K_s \cdot p^L + (2K_s - k^b - k^a) \cdot R \geq 4\underline{\Delta\omega_{qss}} \cdot H \tag{3.26}$$

When total inertia H is constant, the QSS constraint can be solved as

$$p^L = \frac{(2K_s - k^b - k^a) \cdot R - 4\underline{\Delta\omega_{qss}} \cdot H}{2K_s} \tag{3.27}$$

3.3. Pricing Model

As mentioned in subsection 2.1.5, dual values are only available in the solution of ED or SCED but not in the UC or SCUC algorithm. However, SCED gets the same dispatch results as SCUC based on the unit commitment status calculated from the SCUC. Figure 2.2 visualizes this required connection. Among three pricing models introduced in subsection 2.4.3, the restricted model is selected. Different from the “dispatchable model”, this model always gets feasible results. And compared to the “convex hull model”, this model is simpler and requires much less computational burden [22, 23]. By applying the restricted model, there will be extra constraints in the SCED algorithm

$$y_{t,g} = y_{t,g}^{scuc,\star} \quad \forall g \in G, \forall t \in T \qquad \text{(Bridging y between SCUC and SCED)} \tag{3.28}$$

$$x_{t,i} = x_{t,i}^{scuc,\star} \quad \forall (t,i) \in I \qquad \text{(Bridging x between SCUC and SCED)} \tag{3.29}$$

$$z_{t,i} = z_{t,i}^{scuc,\star} \quad \forall (t,i) \in J \qquad \text{(Bridging z between SCUC and SCED)} \tag{3.30}$$

3.4. SCUC and SCED with Flexible FR Bids

After combining the design of the bid structure and other elements of SCUC and SCED discussed in the previous sections, the complete formulation of SCUC and SCED in this project is as follows.

$$\mathcal{P}: \quad \min_{P,y,R,x,H^{vi},z,P^L} \quad C^{fix} + C^{var} + C^{fr} + C^{H}$$

$$= \sum_{t\in T, g\in G}(c_g^{fix}\cdot y_{t,g} + c_g^{var}\cdot P_{t,g}) + \sum_{i,t\in I} c_{t,i}^{fr}\cdot R_{t,i} + \sum_{j,t\in J} c_{t,j}^{H}\cdot H_{t,j}^{vi} \tag{3.31a}$$

Subjected to (s.t.):

(1) Classic UC/ED constraints

$$h^{blz}: \quad \sum_{g\in G} P_{t,g} - d_t = 0 \qquad \forall t\in T \tag{3.31b}$$

$$g^{\underline{P}}: \quad P_{t,g} - y_{t,g}\cdot \underline{P_{t,g}} \geq 0 \qquad \forall t\in T, \forall g\in G \tag{3.31c}$$

$$g^{\overline{P}}: \quad y_{t,g}\cdot \overline{P_{t,g}} - P_{t,g} \geq 0 \qquad \forall t\in T \tag{3.31d}$$

(2) FR Capacity Bounds

$$g^{\underline{R}}: \quad R_{t,i} - x_{t,i}\cdot \underline{R_{t,i}} \geq 0 \qquad \forall (t,i)\in I \tag{3.31e}$$

$$g^{\overline{R}}: \quad x_{t,i}\cdot \overline{R_{t.i}} - R_{t,i} \geq 0 \qquad \forall (t,i)\in I \tag{3.31f}$$

(3) VI Capacity Bounds

$$g^{\underline{H}}: \quad H_{t,j}^{vi} - z_{t,j}\cdot \underline{H_{t,j}^{vi}} \geq 0 \qquad \forall (t,j)\in J \tag{3.31g}$$

$$g^{\overline{H}}: \quad z_{t,j}\cdot \overline{H_{t,j}^{vi}} - H_{t,j}^{vi} \geq 0 \qquad \forall (t,j)\in J \tag{3.31h}$$

(4) the size of the largest unit and FR Sufficiency

$$g^{loss}: \quad P_t^L - P_{t,g} \geq 0 \qquad \forall t\in T, \forall g\in G \tag{3.31i}$$

$$g^{\sum R}: \quad \sum_{i\in I_t} R_{t,i} - P_t^L \geq 0 \qquad \forall t\in T \tag{3.31j}$$

(5) Frequency Constraints

$$g^{RoCoF}: \quad -P_t^L - 2\underline{\omega'}H_t \geq 0 \qquad \forall t\in T \tag{3.31k}$$

$$g^{Nadir}: \quad -k\cdot p_t^L + \sum_{i\in I_t} R_{t,i}\cdot FR_{t,i}(k) - 2\underline{\Delta\omega}H_t \geq 0 \qquad \forall t\in T, \forall k\in K \tag{3.31l}$$

$$g^{qss}: \quad -K_s\cdot p_t^L + \sum_{i\in I_t} R_{t,i}\cdot FR_{t,i}(K_s) - 2\underline{\Delta\omega_{qss}}H_t \geq 0 \qquad \forall t\in T \tag{3.31m}$$

(6) Additional Constraints in SCED (Bridging SCUC and SCED, i.e., "Restricted Pricing Model")

$$h^{y}: \quad y_{t,g} = y_{t,g}^* \qquad \forall t\in T, \forall g\in G \tag{3.31n}$$

$$h^{x}: \quad x_{t,i} = x_{t,i}^* \qquad \forall (t,i)\in I \tag{3.31o}$$

$$h^{z}: \quad z_{t,j} = z_{t,j}^* \qquad \forall (t,j)\in J \tag{3.31p}$$

where K_s is the last time step in the dynamic simulation; $x_{t,i}^*$, $y_{t,g}^*$, and $z_{t,g}^*$ are the solutions of $x_{t,i}$, $y_{t,g}$, and $z_{t,j}$ in the SCUC problem; $FR_{t,i}$ is the integral of the activation curve of each FR product ($fr_{t,i}$); and H_t represents the total inertia at each market period t, including physical inertia and virtual inertia (VI), as shown in the following expression,

$$H_t = \sum_{g\in G} y_{t,g}\cdot H_{t,g} + \sum_{j\in J[t]} H_{t,j}^{vi} \quad \forall t\in T \tag{3.32}$$

Table 3.4 reformulates the SCUC and SCED problem (Equation 3.31) in the format of a matrix of parameters of decision variables. Each column represents a set of decision variables and each row represents a set of constraints. Each entry in the table represents the parameter to a set of decision variables in a set of constraints. Sometimes, the dimension of the set of decision variables is larger than the dimensions of the set of constraints. Sometimes they are equal to each other, and sometimes it is the reverse. In each case, the entry corresponds to the parameters of each single decision variable

in each single constraint in a different way:

- When the dimensions of the set of decision variables (column) and the set of constraints (row) are the same, the corresponding item in the formula is simply the product of the decision variable and parameter with the same subscript.
- When there is an extra dimension in the set of constraints (row) than in the set of decision variables (column), the item in the formula is also the product of the decision variable and the parameter though it is the same for each constraint in the constraint set.
- When there is an extra dimension in the set of decision variables (column) than in the set of constraints (row), the item in the formula is the sum of the product of the decision variable and parameter along the extra dimension.

For example, decision variable $R_{t,i}$ (I) has an extra dimension I_t than the constraint g^{nadir} ($T \times K$) and constraint g^{nadir}. Therefore, the item with $R_{t,i}$ becomes $\sum_{i \in I_t} FR_{t,i}(k) R_{t,i}$ in Equation 3.31l. The extra dimension (K) of constraint and parameter $FR_{t,i}(k)$ is automatically included in the set of constraints.

Table 3.4: Calculating shadow prices π of decision variables from dual values λ of constraints. The dimension is also included after each decision variable or dual value.

Variable	$P_{t,g}$	$y_{t,g}$	P_t^L	$R_{t,i}$	$x_{t,i}$	$H_{t,j}^{vi}$	$z_{t,j}$	Const
Dimension	$T \times G$	$T \times G$	T	I	I	J	J	
Objective	c^{var}	c^{fix}	0	c^{fr}	0	c^{H}	0	0
$h^{blz} \mid T$	1	0	0	0	0	0	0	$-d_t$
$g^{\underline{P}} \mid T \times G$	1	$-\underline{P_{t,g}}$	0	0	0	0	0	0
$g^{\overline{P}} \mid T \times G$	-1	$\overline{P_{t,g}}$	0	0	0	0	0	0
$g^{\underline{R}} \mid I$	0	0	0	1	$-\underline{R_{t,i}}$	0	0	0
$g^{\overline{R}} \mid I$	0	0	0	-1	$\overline{R_{t,i}}$	0	0	0
$g^{\underline{H}} \mid J$	0	0	0	0	0	1	$-\underline{H_{t,j}^{vi}}$	0
$g^{\overline{H}} \mid J$	0	0	0	0	0	-1	$\overline{H_{t,j}^{vi}}$	0
$g^{loss} \mid T \times G$	-1	0	1	0	0	0	0	0
$g^{\sum R} \mid T$	0	0	-1	1	0	0	0	0
$g^{RoCoF} \mid T$	0	$-2\underline{\omega'} H_{t,g}$	-1	0	0	$-2\underline{\omega'}$	0	0
$g^{nadir} \mid T \times K$	0	$-2\underline{\Delta\omega} H_{t,g}$	$-k$	$fr_{t,i}[k]$	0	$-2\underline{\Delta\omega}$	0	0
$g^{QSS} \mid T$	0	$-2\underline{\Delta\omega_{qss}} H_{t,g}$	$-K_s$	$fr_{t,i}[K_s]$	0	$-2\underline{\Delta\omega_{qss}}$	0	0
$h^{y} \mid T \times G$	0	1	0	0	0	0	0	$-y_{t,g}^*$
$h^{x} \mid I$	0	0	0	0	1	0	0	$-x_{t,i}^*$
$h^{z} \mid J$	0	0	0	0	0	0	1	$-z_{t,j}^*$

Table 3.4 is not only a summary of the primal problem, as formulated in Equation 3.31, but also the constraints in the dual problem, as formulated in Table 3.5.

Table 3.5: Constraints in the dual problem

$$
\begin{aligned}
\pi^{P}_{t,g}: \quad & c^{var}_{t,g} = \lambda^{blz}_{t} + \lambda^{\underline{P}}_{t,g} - \lambda^{\overline{P}}_{t,g} - \lambda^{loss}_{t,g} \\
\pi^{y}_{t,g}: \quad & c^{fix}_{t,g} = -\underline{P_{t,g}}\lambda^{\underline{P}}_{t,g} + \overline{P_{t,g}}\lambda^{\overline{P}}_{t,g} - 2\underline{\omega'}H_{t,g}\lambda^{RoCoF}_{t} - 2\underline{\Delta\omega}H_{t,g}\sum_{k\in K}\lambda^{nadir}_{t,k} - 2\underline{\Delta\omega_{qss}}H_{t,g}\lambda^{qss}_{t} + \lambda^{y}_{g,t} \\
\pi^{P^L}_{t}: \quad & 0 = \sum_{g\in G}\lambda^{loss}_{t,g} - \lambda^{\sum R}_{t} - \lambda^{RoCoF}_{t} - \sum_{k\in K} k\cdot\lambda^{nadir}_{t,k} - K_s\cdot\lambda^{qss}_{t} \\
\pi^{R}_{t,i}: \quad & c^{fr}_{t,i} = \lambda^{\sum R}_{t} + \lambda^{\underline{R}}_{t,i} - \lambda^{\overline{R}}_{t,i} + \sum_{k\in K} fr_{t,i}[k]\cdot\lambda^{nadir}_{t,k} + fr_{t,i}[K_s]\cdot\lambda^{QSS}_{t} \\
\pi^{x}_{t,i}: \quad & 0 = -\underline{R_{t,i}}\cdot\lambda^{\underline{R}}_{t,i} + \overline{R_{t,i}}\cdot\lambda^{\overline{R}}_{t,i} + \lambda^{x}_{t,i} \\
\pi^{H}_{t,j}: \quad & c^{H}_{t,j} = \lambda^{\underline{H}}_{t,j} - \lambda^{\overline{H}}_{t,j} - 2\underline{\omega'}\cdot\lambda^{RoCoR}_{t} - 2\underline{\Delta\omega}\sum_{k\in K}\lambda^{nadir}_{t,k} - 2\underline{\Delta\omega_{qss}}\cdot\lambda^{QSS}_{t} \\
\pi^{z}_{t,j}: \quad & 0 = -H^{vi}_{t,j}\cdot\lambda^{\underline{H}}_{t,j} + H^{vi}_{t,j}\cdot\lambda^{\overline{H}}_{t,j} + \lambda^{z}_{t,j}
\end{aligned}
$$

In the next chapter, we will use two study cases to analyze the patterns of dependency when applying this SCUC/SCED formulation to cases where there is only one type of FR dynamics.

4

Case study

To have an understanding of the patterns of dependencies in the proposed SCUC and SCED formulation, in this project, we will analyze the simplest scenarios, where there is only one type of FR dynamics. We will focus on the relationship between the amount of FR or VI sold and the bid price of FR or VI. The first section will discuss the test network that is used in the case study. The second section will provide an overview of the case study. Then, the size of the simulation time step is selected before we go into the results and analysis.

4.1. Test Network Setups

We run the study cases on Gurobi 10.0.3 [26]. The coding is on Python 3.11.0 with Jupyter Notebook [27]. The network models, parameters, and other general setups are discussed in this section.

4.1.1. IEEE 24-Bus Reliability Test System

In this project, study cases are run on a test network with one node that scales up the IEEE 24-bus reliability test system (RTS) [28]. Table 4.1 provides an overview of generation units in the original test system. There are 31 generation units with a total installed capacity of 3.208 GW. To guarantee equal opportunity of dispatching, we only consider variable costs of each generation unit while ignoring fixed costs.

4.1.2. Adapting the test case to this project

In this project, there are some modifications to the original IEEE 24-bus RTS for simplicity and better visualization. Firstly, the fuel types and inertia constants of each generation unit are re-assigned based on the size of generation units, i.e., their installed capacity. The columns of Table 4.1 are explained as follows together with the rules to categorize generation units:

- $Fuel$: Fuel type of each generation unit. In this project, the original fuel types of units are not used. For simplicity, one of five fuel types is assigned to each unit based on its generation capacity. Each unit in the graph for dispatch results, such as Figure 2.1, is colored based on its fuel type to enhance visualization. Moreover, the inertia constants H of units are assigned based on fuel

Table 4.1: Generation units in IEEE 24-bus Reliability Test System (RTS). For simplicity, fuel types are re-assigned based on generation capacities, and inertia values are adjusted based on assigned fuel types. In this project, the IEEE 24-bus RTS is duplicated eight times to mimic a medium-sized grid with a total installed capacity of 25.664 GW. The fixed cost is not considered in this project and is assumed to be zero to remove its influence on the dispatch result.

Name	Fuel	$H\ [s]$	$\underline{P}\ [MW]$	$\overline{P}\ [MW]$	c^{var} [€/MWh]
gen00	Gas	2.8	16	20	130
gen01	Gas	3	15.2	76	16.0811
gen02	Gas	3	15.2	76	16.0811
gen03	Gas	2.8	16	20	130
gen04	Gas	3	15.2	76	16.0811
gen05	Gas	3	15.2	76	16.0811
gen06	Coal	2.8	25	100	43.6615
gen07	Coal	2.8	25	100	43.6615
gen08	Coal	2.8	69	197	48.5804
gen09	Coal	2.8	69	197	48.5804
gen10	Hydro	2.8	2.4	12	56.564
gen11	Hydro	2.8	2.4	12	56.564
gen12	Hydro	2.8	2.4	12	56.564
gen13	Hydro	2.8	2.4	12	56.564
gen14	Coal	3	54.3	155	12.3883
gen15	Gas	3.5	10	50	0.001
gen16	Gas	3.5	10	50	0.001
gen17	Gas	3.5	10	50	0.001
gen18	Gas	3.5	10	50	0.001
gen19	Gas	3.5	10	50	0.001
gen20	Coal	3	54.3	155	12.3883
gen21	Coal	3	140	350	11.8495
gen22	Gas	2.8	16	20	130
gen23	Gas	2.8	16	20	130
gen24	Coal	2.8	25	100	43.6615
gen25	Hydro	2.8	2.4	12	56.564
gen26	Coal	3	54.3	155	12.3883
gen27	Nuclear	5	100	400	4.4231
gen28	Nuclear	5	100	400	4.4231
gen29	Gas	3.5	10	50	0.001
gen30	Coal	3	54.3	155	12.3883

type.:

$$Fuel = \begin{cases} Nuclear & H = 5\ s & \text{(Ochre)} & \text{if } \overline{P} \geq 400 \text{ MW} \\ Coal & H = 3\ s & \text{(Grey)} & \text{if } 100 \leq \overline{P} < 400 \text{ MW} \\ Gas & H = 2.8\ s & \text{(Purple)} & \text{if } 15 \leq \overline{P} < 100 \text{ MW} \\ Hydro & H = 3.5\ s & \text{(Dark Blue)} & \text{if } 0 < \overline{P} < 15 \text{ MW and } \underline{P} \neq 0 \\ Wind & H = 0\ s & \text{(not visible)} & \text{if } 0 < \overline{P} < 15 \text{ MW and } \underline{P} = 0 \end{cases}$$

- H: inertia constant of each generation unit, which is assigned on the rule described above.
- $\underline{P}$: minimum stable generation (MSG), which is the lower bound limit for generation capacity.
- $\overline{P}$: installed capacity, which is the upper bound limit of generation capacity.
- c^{var}: variable cost, or fuel cost. It is the price per megawatt (MW) of energy dispatched.

The IEEE 24-bus RTS represents a small grid. In this project, the context of analysis is on a medium-size grid. Therefore, we scaled up the original test case by eight times. Each generation unit in Table 4.1 is duplicated and the total installed capacity in study cases is 25.664 GW.

4.1.3. Basic parameters in study cases

Table 4.2 summarizes some common parameters used in all study cases. The nominal frequency is selected as $f_0 = 50$ Hz. The active power corresponding to one per unit equals to the total installed generation capacity in the network, which is 25.664 GW. The frequency requirements are chosen as -0.25 Hz for the frequency nadir limit, -1 Hz/s for the RoCoF limit, and -0.15 Hz for the QSS limit. The load level is chosen as 0.8 per unit, which corresponds to 20.531 GW.

Table 4.2: Basic parameters used in study cases

Parameter	Symbol	Value	Per unit value
Nominal frequency	f_0	50 Hz	1
Per unit active power	$P^{p.u.}$	25.664 GW	1
Total installed generation capacity	P^{tot}	25.664 GW	1
Frequency nadir limit	$\Delta\omega_{min}$	-0.25 Hz	-0.005
RoCoF limit	ω'_{min}	-1 Hz/s	-0.02/s
QSS limit	$\Delta\omega_{qss}$	-0.15 Hz	-0.003
Load	d	20.531 GW	0.8

4.2. Cases Study Overview and Setups

Before going into study cases and their results, in section 4.3 we will first select the appropriate time step dk for dynamic simulations in the SCUC and SCED. All study cases will then apply this time step in the algorithms.

There are five study cases in this project. Table 4.3 provides an overview of parameters used in each case study. Every case study consists of several multi-period SCUC and SCED problems (i.e., “sub-problems”) with different FR bids and inertia bids at each market period of each sub-problem. In

each market, only one bid is considered for simplicity. There are eight parameters in FR and inertia bids. In each study case, each of these parameters are assigned different roles, among which are

- *independent variable*, denoted as "**X**", which selects different sample values at each market period t but the same across sub-problems,
- *dependent variable*, denoted as "**Y**", which is one of the targets for analysis, the variable is usually the amount of FR or VI, which will be set to positive infinity ($+\infty$ to remove any external constraint on the SCUC and SCED results).
- *sampling variable*, denoted as "**S**", which selects a different value for each sub-problem but keeps constant in different market periods within a sub-problem and corresponds to different series of "Y-X" curves in order to see whether the sampling variable influences the pattern, as well as
- several *control variables*, which remain constant in all market periods and all sub-problems.

Table 4.3: Overview of study cases in this project. In each case study, there is an *independent variable*, indicated by "**X**", and plotted on the x-axis of the resulting graph; a *dependent variable*, indicated by "**Y**", and plotted on the y-axis of the resulting graph; a *sampling variable* for different data series, indicated by "**S**", and shown in the legend. Constants in the tables are *control variables*.

Study Case	FR bids					Inertia bids		
	k^a	k^b	$\overline{R}$	c^{fr}	Flex?	$\overline{H}$	c^H	Flex?
0. Select dk	3	8	**Y**	**X**	✓	0	-	-
1. $R - c^{fr}$	3	8	**Y**	**X**	✓	**S**	1	*x*
2. $H_{vi} - c^H$	3	8	**S**	100	*x*	**Y**	**X**	✓
4. $H_{vi} - R$	3	8	**X**	100	*x*	**Y**	**S**	✓

The two study cases in this project will examine the dependency between the amount of FR or VI sold and the price of the same product when there is only one FR dynamic. Before that, a preparatory study case will be conducted to choose the most suitable simulation time step for those two main study cases.

4.2.1. Setup of Case 0: Selection of Simulation Time Step

Study case 0 studies the impact of simulation resolution on the quality of simulation results. After balancing the quality of results and computational burden, we select the most appropriate time step dk for other study cases in this project.

There are three indicators in the selection of dk. The first one is the quality of simulation results, which can be observed from the smoothness of the curve which is supposed to be smooth theoretically. In other words, an appropriate value of the time step will make sure that the result of the optimization problem replicates the actual patterns, i.e., the smoothness of an inherently smooth curve. The second one is the marginal improvement in quality. If there is no apparent improvement when the time step is further reduced, then we consider the previous dk as optimal. The third one is the computational burden. The time to run the algorithm is almost inversely proportional to the time step dk. Therefore, the selection of dk needs to be balanced with the computational burden. The dependency between the amount of FR and the price of FR is inherently smooth, therefore, it is selected as a showcase in this section. The independent variable "**X**" is the price of FR, and the dependent variable "**Y**" is the FR demand. Table 4.4 shows the FR bids in this study case. We consider one single FR product for

simplicity and set its feature as flexible and the bid amount as infinity so that there are no external limitations to FR demand, and thus the procurement is only responsive to FR price. We select the time delay of the FR product as $k^a = 3$ s and the time of full delivery $k^b = 8$ s. In the virtual inertia market, no inertia bid is considered for simplicity. The sampling variable ("**S**") in this study case is the time step dk, which is selected as 0.05 s, 0.02 s, 0.01 s, 0.002 s, and 0.001 s as summarized in Table 4.5.

Table 4.4: FR Bids in study case 0. The purpose is to compare the quality of simulation results with time steps and select the most appropriate time step for study cases in this project. The same SCUC and SCED are run five times with different simulation time steps dk as *sampling variables ("**S**"), which are 0.001 s, 0.002 s, 0.01 s, 0.02 s, and 0.05 s.*

Market period t	Provider i	k^a $[s]$	k^b $[s]$	$\overline{R}$ $[MW]$	c^{FR} $[€/MW{\cdot}h]$	Flexible?
1	Wind 1	3	8	$+\infty$	$10^0 = 1$	True
2	Wind 1	3	8	$+\infty$	$10^{0.01}$	True
3	Wind 1	3	8	$+\infty$	$10^{0.02}$	True
...	...	...	...	...	...	...
49	Wind 1	3	8	$+\infty$	$10^{0.48}$	True
50	Wind 1	3	8	$+\infty$	$10^{0.49}$	True
51	Wind 1	3	8	$+\infty$	$10^{0.5} = \sqrt{10}$	True

Table 4.5: Sampling parameters ("S") of sub-problems in study case 1. The influence of the amount of virtual inertia (VI) on the dependency between the amount of FR and the price of FR.

Sub-problem	Simulation Time Step [s]
1	0.05
2	0.02
3	0.01
4	0.002
5	0.001

4.2.2. Setup of Case 1: Dependency Between FR Amount and Bid Price

In this study case, we will answer the question of what the pattern of dependency is between the amount of FR and the price of FR, as well as the dependency between the size of the largest unit and the amount of FR needed.

For simplicity, we only consider one single flexible FR product with a delay of $k^a = 3$ s and delivery time of $k^b - k^a = 5$ s. We sample the price of FR from 1 €/MW-h to 10,000 €/MW-h in a logarithmic scale and set the upper bound (amount of FR in bid) of the FR product to positive infinity to remove the external bound. To check the influence of the amount of VI on the dependency between FR price and FR amount, the SCUC and SCED are run four times, once per sub-problem, with different levels of VI. Table 4.6 summarizes the input values, i.e., FR bids, into the SCUC and SCED optimization problem in every sub-problem, and Table 4.8 summarizes the amount of VI in each sub-problem.

Table 4.6: FR Bids in the study case 1 to analyze the dependency between the amount of FR and the price of FR. The price of FR is the independent variable ("**X**"), which is assigned different values for each market period but has the same pattern of time-dependence across sub-problems. The amount of VI is the sampling variable ("**S**"), and Table 4.8 summarizes the choices of its value in each sub-problem. It remains constant within each sub-problem. The available FR ($\overline{R}$) is set as infinite and the product is set as flexible to remove any external bound for the FR demand. The price of FR (c^{fr}) is the control variable and remains constant at 100 €/MW-h in all bids.

Market period t	Provider i	k^a $[s]$	k^b $[s]$	$\overline{R}$ $[MW]$	c^{FR} $[€/MW{\cdot}h]$	Flexible?
1	Wind 1	3	8	$+\infty$	$X_1 = 10^0$	True
2	Wind 1	3	8	$+\infty$	$X_2 = 10^{0.04}$	True
3	Wind 1	3	8	$+\infty$	$X_3 = 10^{0.08}$	True
...	...	...	...	...	...	...
99	Wind 1	3	8	$+\infty$	$X_{49} = 10^{3.92}$	True
100	Wind 1	3	8	$+\infty$	$X_{50} = 10^{3.96}$	True
101	Wind 1	3	8	$+\infty$	$X_{51} = 10^4$	True

Table 4.7: VI Bids in study case 1 to analyze the dependency between the amount of FR and the price of FR.

Market period t	Provider i	$\overline{H_{vi}}$ $[MW]$	c^H $[€/MW{\cdot}h]$	Flexible?
1	Wind 2	S_i	1	True
2	Wind 2	S_i	1	True
3	Wind 2	S_i	1	True
...	...	...	...	...
99	Wind 2	S_i	1	True
100	Wind 2	S_i	1	True
101	Wind 2	S_i	1	True

Table 4.8: Sampling parameters ("S") of sub-problems in study case 1. The purpose of the sampling parameters is to explore the influence of the amount of virtual inertia (VI) on the dependency between the amount of FR and the price of FR.

Sub-problem	Amount of VI [s]	Amount of VI [MW-h]	Price of VI [€/MW-h]
1	0.1	2,566.4	1
2	1	25,664	1
3	3	76,992	1
4	10	256,640	1

4.2.3. Setup of Case 2: Dependency Between VI Amount and Bid Price

In this study case, we will answer the question of what the pattern of dependency is between the amount of VI and the price of VI.

In the VI bids, we consider one single flexible VI product and sample the price of VI from 0 €/MW-s to 4 €/MW-s with 100 samples on a linear scale in different market periods. In the FR bids, we set the price of FR constant at $c^{fr} = 100$ €/MW-h, and the amount of FR at different constant levels for

different sub-problems. Table 4.9 summarizes the bids of FR in each market period. And Table 4.10 summarizes the bids of VI in each market period. The independent variable ("**X**") is the price of virtual inertia (c^H) and the sampling variable is the amount of frequency response ($\overline{R}$). The control variable is the price of frequency response (c^{fr}). In each sub-problem, we choose different values of sampling variables ("**S**"), which is summarized in Table 4.11.

Table 4.9: FR in Study Case 2. The purpose is to analyze the dependency between the amount of VI and the price of VI. We select the amounts of FR as the *sampling variables* ("**S**") and keep the price of FR constant at 100 €/MW-h.

Market period t	Provider i	k^a $[s]$	k^b $[s]$	$\overline{R}$ $[MW]$	c^{FR} $[€/MW{\cdot}h]$	Flexible?
1	Wind 1	3	8	S_i	100	False
2	Wind 1	3	8	S_i	100	False
3	Wind 1	3	8	S_i	100	False
...	...	...	...	...	...	...
99	Wind 1	3	8	S_i	100	False
100	Wind 1	3	8	S_i	100	False
101	Wind 1	3	8	S_i	100	False

Table 4.10: FR in Study Case 2. The purpose is to analyze the dependency between the amount of VI and the price of VI. We choose the price of VI as the independent variable ("**X**"). We choose the amount of VI as the dependent variable ("**Y**") and keep the bid amount at positive infinity to remove any external constraints on the SCUC and SCED results.

Market period t	Provider i	$\overline{H_{vi}}$ $[MW]$	c^H $[€/MW{\cdot}h]$	Flexible?
1	Wind 2	$+\infty$	$X_1 = 0$	False
2	Wind 2	$+\infty$	$X_2 = 0.04$	False
3	Wind 2	$+\infty$	$X_3 = 0.08$	False
...	...	...	...	...
99	Wind 2	$+\infty$	$X_{99} = 3.92$	False
100	Wind 2	$+\infty$	$X_{100} = 3.96$	False
101	Wind 2	$+\infty$	$X_{101} = 4$	False

Table 4.11: Sampling parameters ("S") of sub-problems in study case 2. The influence of the amount of frequency response (FR) on the dependency between the amount of VI and the price of VI.

Sub-problem	Amount of FR [MW]	Price of FR [€/MW-h]
1	300	100
2	500	100
3	1000	100
4	3000	100

4.2.4. Setup of Case Study 3: Dependency Between the Amount of VI and the Amount of FR

In this study case, we will answer the question of what the pattern of dependency is between the amount of VI and the amount of FR. In each market period, we choose different values for the amount of FR, which is the independent variable ("**X**"), from 250 MW to 1,250 MW with 100 intervals on a linear scale. We set the price of VI constantly at 1 €/MW-s as the control variable and the amount of VI constantly at positive infinity to remove any external constraints on the amount of VI. In each sub-problem, we choose a different price of FR, as the *sampling variable* ("**S**"). Table 4.12 summarizes the bids of frequency response at each market period, and Table 4.13 summarizes the bids of virtual inertia at each market period. Table 4.14 shows different values chosen for the price of FR in each sub-problem.

Table 4.12: FR Bids in study case 5. The purpose is to analyze the pattern of dependency between the amount of VI and the amount of FR. We select the amount of FR as the independent variable ("**X**"), which is sampled from 250 MW to 1250 MW on a linear scale. We also select the price of FR as the sampling variable ("**S**"), which has the same value at different market periods within a sub-problem but different values in different sub-problems.

Market period t	Provider i	k^a $[s]$	k^b $[s]$	$\overline{R}$ $[MW]$	c^{FR} $[€/MW{\cdot}h]$	Flexible?
1	Wind 1	3	8	$X_1 = 250$	S_i	False
2	Wind 1	3	8	$X_2 = 260$	S_i	False
3	Wind 1	3	8	$X_3 = 270$	S_i	False
...	...	...	...	...	...	...
99	Wind 1	3	8	$X_{49} = 1230$	S_i	False
100	Wind 1	3	8	$X_{50} = 1240$	S_i	False
101	Wind 1	3	8	$X_{51} = 1250$	S_i	False

Table 4.13: VI Bids in study case 5. The purpose is to analyze the pattern of dependency between the amount of VI and the amount of FR. We select the amount of VI as the dependent variable ("**Y**"), which is kept constant at positive infinity to remove any external constraints on the result of SCUC and SCED. We keep the price of VI constant at 1 €/MW-h.

Market period t	Provider i	$\overline{H_{vi}}$ $[MW]$	c^H $[€/MW{\cdot}h]$	Flexible?
1	Wind 2	$+\infty$	1	True
2	Wind 2	$+\infty$	1	True
3	Wind 2	$+\infty$	1	True
...	...	...	...	...
99	Wind 2	$+\infty$	1	True
100	Wind 2	$+\infty$	1	True
101	Wind 2	$+\infty$	1	True

Table 4.14: Sampling parameters ("S") of sub-problems in study case 5. The influence of the price of virtual inertia (VI) on the dependency between the amount of VI and the amount of FR.

Sub-problem	Amount of VI [MW-h]	Price of VI [€/MW-h]
1	$+\infty$	0.1
2	$+\infty$	0.5
3	$+\infty$	1.0
4	$+\infty$	2.0

4.3. Results of Study Case 0: Selection of Simulation Time Steps

Figure 4.1 shows that the selection of the time step has a significant impact on the validity of simulation results. When the time step dk is as large as 0.05 s, as represented by the black curve, the result is far from the theoretical pattern and with severe granularity. The curve becomes more smooth with decreasing time steps. When the time step dk is 0.001 s, as represented by the dashed pink line, the curve is almost smooth with only minor fluctuation. However, it does not differ much from the curve for the time step of 0.002 s, as represented by the dashed purple line. Moreover, with a time step of 0.002 s, it requires only about half the time to run the algorithm. Therefore, considering the balance between the quality of simulation results and the computational burden, we choose $dk = 0.002$ s for the study cases in this project.

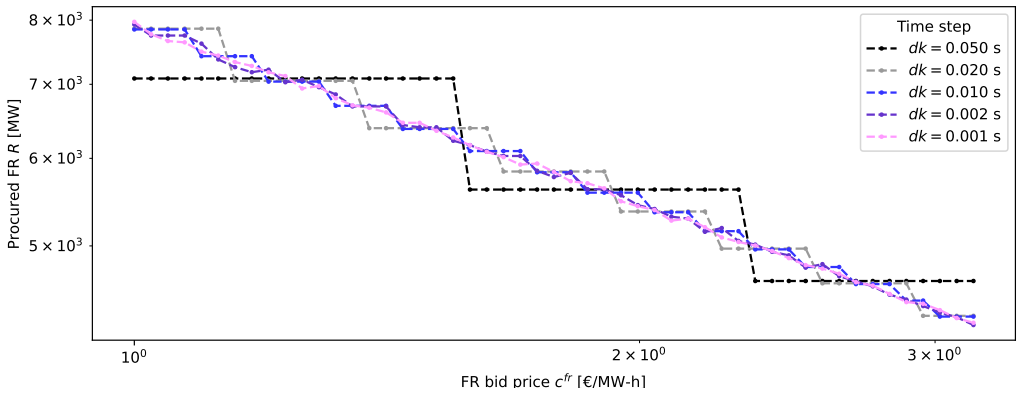

Figure 4.1: The smoothness of the curve when the time resolution of dynamic simulation in the SCUC and SCED is chosen at different values. With large time steps, the result shows obvious granularity. For example, when $dk = 0.05$ s, as represented by the black curve, the curve is significantly discrete. The granularity decreases with the finer time step. When $dk = 0.002$ s, the curve is almost smooth, which is close to the actual pattern. When the time step is even smaller, i.e., when $dk = 0.001$ s, the granularity only improves a little while almost doubling the computational burden. Therefore, we select $dk = 0.002$ s as the time step for all other study cases.

The requirement of the simulation time step is higher than in the work by Xu et. al [20], which also performs a numerical simulation for frequency dynamics inside the SCUC and SCED. Figure 4.2 explains the reason why there is granularity in the curve of an inherently smooth pattern. The first figure shows the time of reaching the frequency nadir in response to the change in FR price, and the second figure shows the frequency dynamics in each market period of each sub-problem. In each sub-problem, there are 51 market periods, corresponding to 51 FR prices, which are visualized in the same color. Theoretically, when the price of FR increases, the demand for FR decreases smoothly, and thus the frequency dynamics change marginally. However, when the simulation time step is large, such

change is highly discrete. For example, when the time step is increased to $dk = 0.05$ s, as represented by the black curve, a bundle of curves is reduced to only three curves, whose corresponding k_{nadir} is the only "existing basket" for adjacent k_{nadir} values due to its discreteness, and thus the result is very different from the actual one. In contrast, the result when the simulation time step is $dk = 0.001$ s is highly flexible. The frequency dynamics change with the FR price smoothly, resulting in a bundle of frequency curves, as represented by thin purple lines. When the time step is increased to $dk = 0.002$ s, as shown in the dashed blue line, there is some degree of discreteness and the number of frequency curves decreases. However, the curve of time of frequency nadir is already close to a smooth curve.

In summary, we select $dk = 0.002$ s for the study cases in this project because it replicates the smooth curve very well and converges to the best performance while balancing well with the computational burden.

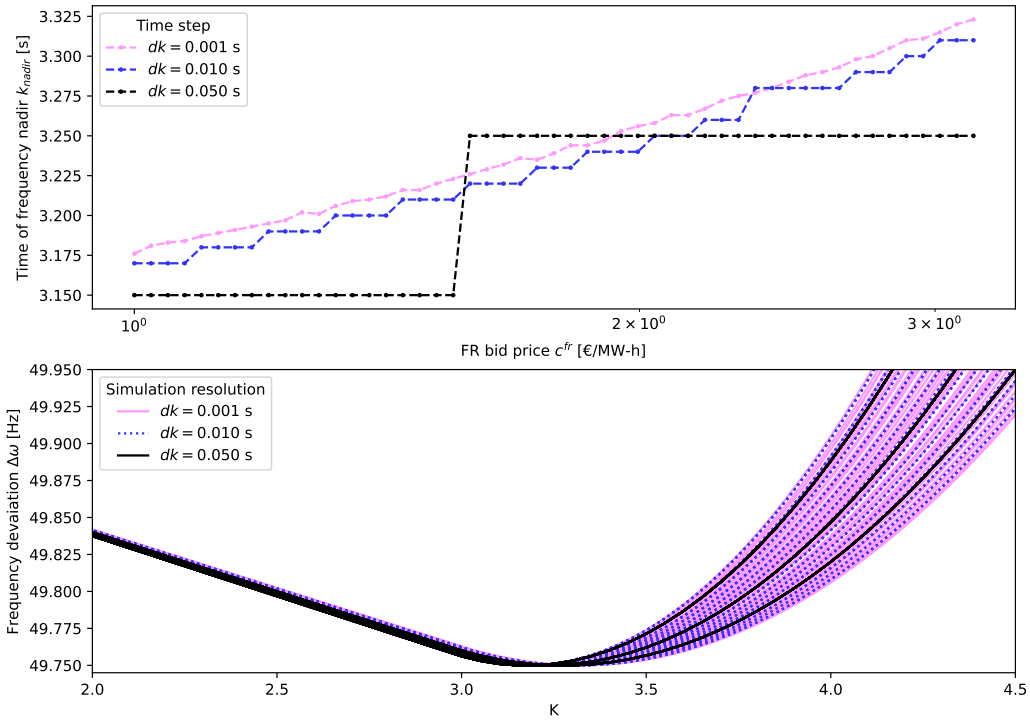

Figure 4.2: Time of reaching frequency nadir and frequency dynamics in each market period in each sub-problem. The first graph shows that the granularity mainly comes from the discreteness of simulation time k. When the time step dk is as large as 0.05 s there are two different times of frequency nadir k_{nadir}. The second curve shows that this is not the expected result but rather due to the granularity of the time step. When the time step dk is short, the FR price changes the frequency dynamics smoothly. However, when the time step is longer, the results in the case of different FR prices group together due to the granularity of dk.

4.4. Results of Study Case 1: Dependency Between Amount of FR and Price of FR

The dependency between the amount of FR sold and the bid price of FR is shown in Figure 4.3. The large circle marker indicates that the binding constraint is the frequency nadir constraint, and the small round marker indicates that the binding constraint is the QSS constraint. When both constraints are

binding, it is indicated by a large circle filled with a small round marker. In general, there are three distinctive patterns in the graph.

When the FR bid price is low and the amount of VI is high, such as the left half of the blue and the purple curve, the amount of FR sold remains constant, regardless of the binding frequency constraint. When the price is higher, the curve either is bonded by the QSS constraint or shows a similar pattern as low-inertia ones, such as the blue curve when the price is between 60 and 100 €/MW-h.

When the amount of VI is small, the nadir constraint is binding when the price of FR is low (less than around 200 €/MW-h). The amount of FR decreases with the increasing price of FR at an almost constant rate on the logarithmic scale.

When the price of FR is high, all sub-problems show similar patterns. They are all bonded by the QSS constraint or no constraint is binding, discretely dependent on the price of FR, and kept constant when the price is higher than around 2000 €/MW-h.

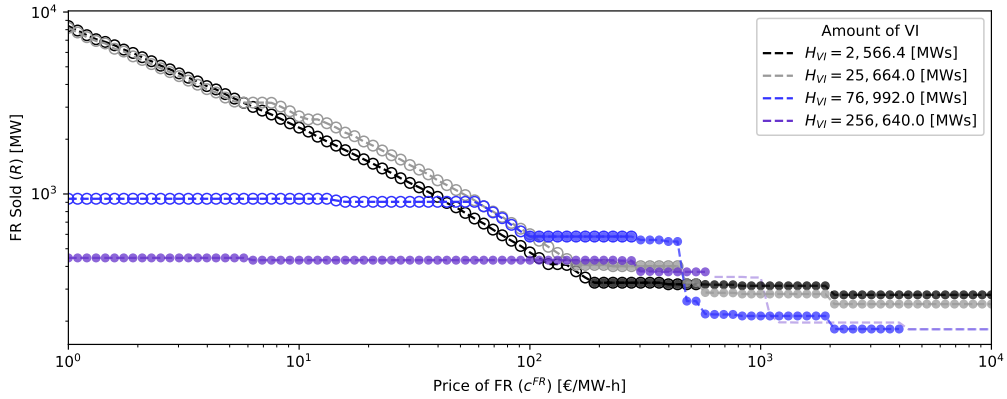

Figure 4.3: Dependency between FR price and FR amount when there is different virtual inertia available. The circle marker indicates that the frequency nadir constraint is binding, and the small round marker indicates that the QSS constraint is binding. The large round marker indicates that both the QSS and the nadir constraint are binding. The RoCoF constraint is never binding in the selected case study. The lines become thin and transparent when none of the frequency constraints are binding

The dependency between the active power of the largest dispatched unit (i.e., “the size of the largest unit”), as shown in Figure 4.4, has similar patterns as Figure 4.3. The parts where the amount of FR remains constant are also where the size of the largest unit remains constant at its maximum value (i.e., 400 MW, which is the installed capacity of the largest unit). Otherwise, when only the nadir constraint is binding, both FR and the size of the largest unit decrease smoothly with increasing FR price till that the QSS is binding. The size of the largest unit also changes step-wise with regards to the bid price FR when the QSS constraint or none is binding. The size of the largest unit remains constant at a minimum level when the price of FR is high enough.

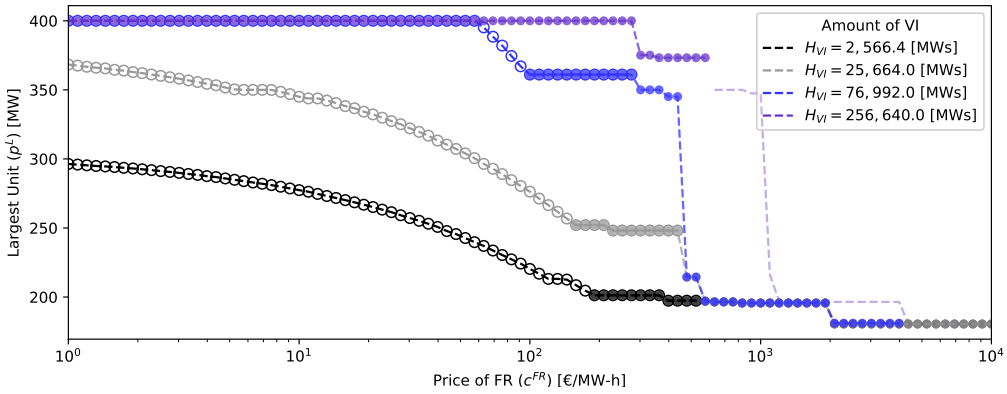

Figure 4.4: Largest power at different FR prices and different VI amounts. When the amount of FR remains constant, the size of the largest unit is also constant. When the nadir constraint is binding, the dependency shows a smooth pattern, and when the QSS is binding, the dependency shows a step-wise pattern.

Figure 4.5 shows the dependence between the size of the largest unit (p^L) and the amount of FR (R). Different patterns show when different frequency constraints are binding. The thin red lines represent the $p^L - R$ relationship derived from the analytical nadir constraint (Equation 3.21) and the thin grey lines represent the $p^L - R$ relationship derived from the analytical QSS constraint (Equation 3.26). Both consider an approximate physical inertia of 3.45 s. Most data points fall on the curve of the corresponding analytical constraint with very little error. Therefore, the analytical expression of the dependencies, i.e., Equation 3.22 and Equation 3.27, confirms the results from the algorithm with the discretized nadir and QSS constraint.

When the size of the largest unit reaches the maximum value (400 MW), the amount of FR sold (as in the case of blue and purple lines) only has an extra increase by a very small amount beyond the curve of the analytical constraint, and does not deviate much from the expected pattern as is described by the thin red and grey lines.

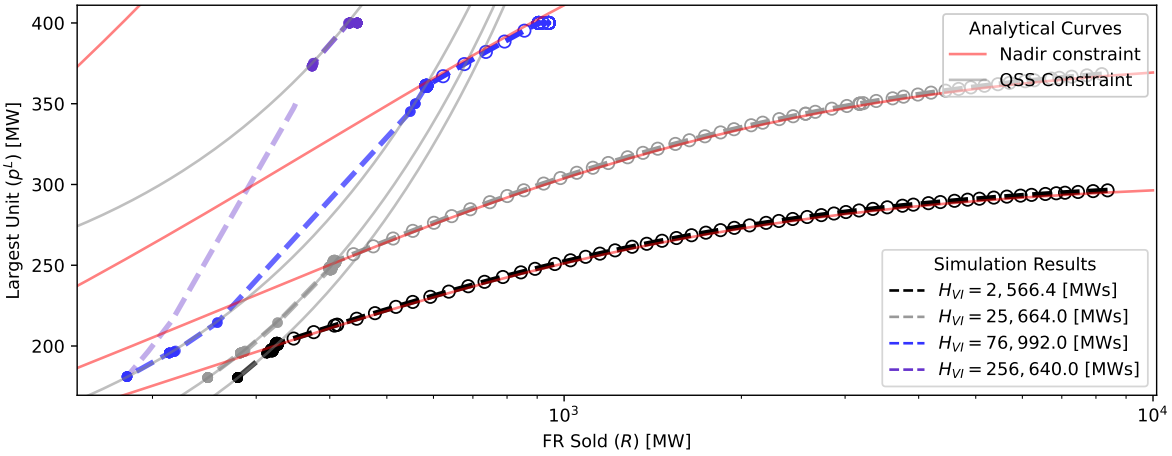

Figure 4.5: Dependence between the size of the largest unit and the amount of FR sold. When different frequency constraint is binding, the dependence shows different patterns. The thin red lines and the thin grey lines are the curves for the analytical nadir constraint and QSS constraint, respectively, when the physical inertia is approximated at 3.5 s for all sub-problems. Nearly all data points of the numerical SCUC and SCED results fall on the corresponding analytical curve.

As shown in Figure 4.6, the size of the largest unit (p^L) has a strong correlation with the total energy costs c^{var}. Theoretically, the total energy cost is decided by the entire combination of dispatched

active powers. The largest unit is only one of them. However, the pattern in Figure 4.6 shows that the largest unit is representative enough for the combination. Moreover, it is a general pattern, which only depends on the network setups and the formulation of the optimization problems and does not change with different FCAS bids or the binding constraints. When frequency nadir is the only binding constraint and the size of the largest unit has not reached the maximum value, the dependency is almost linear.

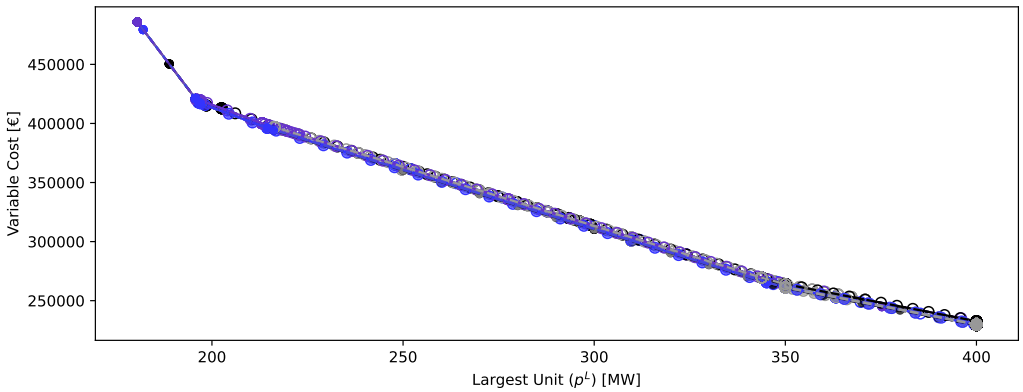

Figure 4.6: The strong correlation between the size of the largest unit p^L and the total variable energy costs c^{var}. This curve holds for every study case, regardless of FR and VI bids or the binding constraint.

When the bid price FR is low, buying a large amount of FR is a better option to mitigate the frequency drop compared to reducing the size of the largest unit, which will induce higher total energy cost, as shown in Figure 4.6. When the FR starts to activate, the frequency stops decreasing within a short time and recovers very fast, as shown in Figure 4.7. For example, when the amount of virtual inertia is 76,992 MWs (equivalent to 3 s) or 256,640 MWs (equivalent to 10 s), the frequency reaches a nadir within around 0.5 seconds after that the FR starts to activate.

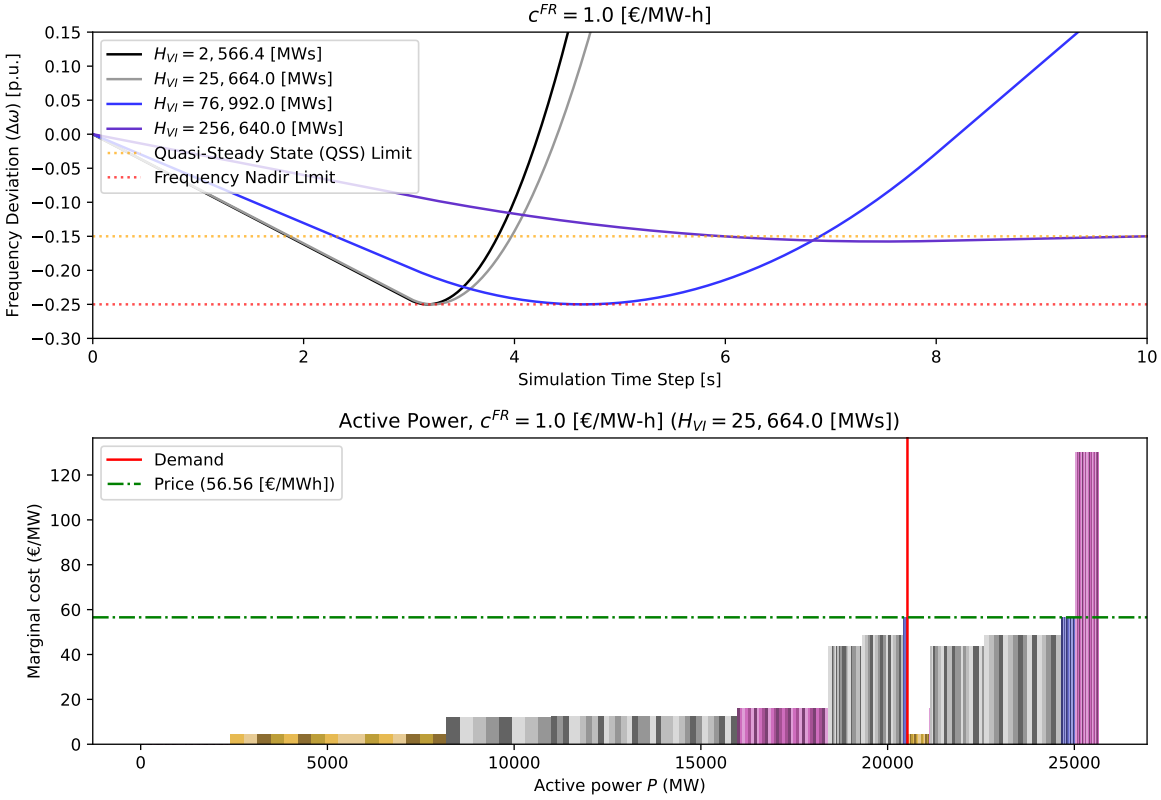

Figure 4.7: Frequency Curve and the Dispatch of Active Power of the Second Sub-Problem When the FR Bid Price is Low. Immediately after the contingency, the RoCoF is relatively large due to the large power imbalance. Once the FR starts to activate, the frequency bounces back from the frequency nadir very fast due to the large amount of FR, especially when the amount of virtual inertia is also low. The dispatch of active power does not deviate from the merit order curve a lot. Only the largest units reduce their output by a small amount and the hydropower plant sets the energy price.

When the price of FR is high, the size of the largest unit is lower, as shown in Figure 4.8, because it is a better option to mitigate the frequency drop compared to procuring more FR. As a result, the RoCoF is much lower; the frequency drops and recovers slower and the QSS constraint is binding for all sub-problems.

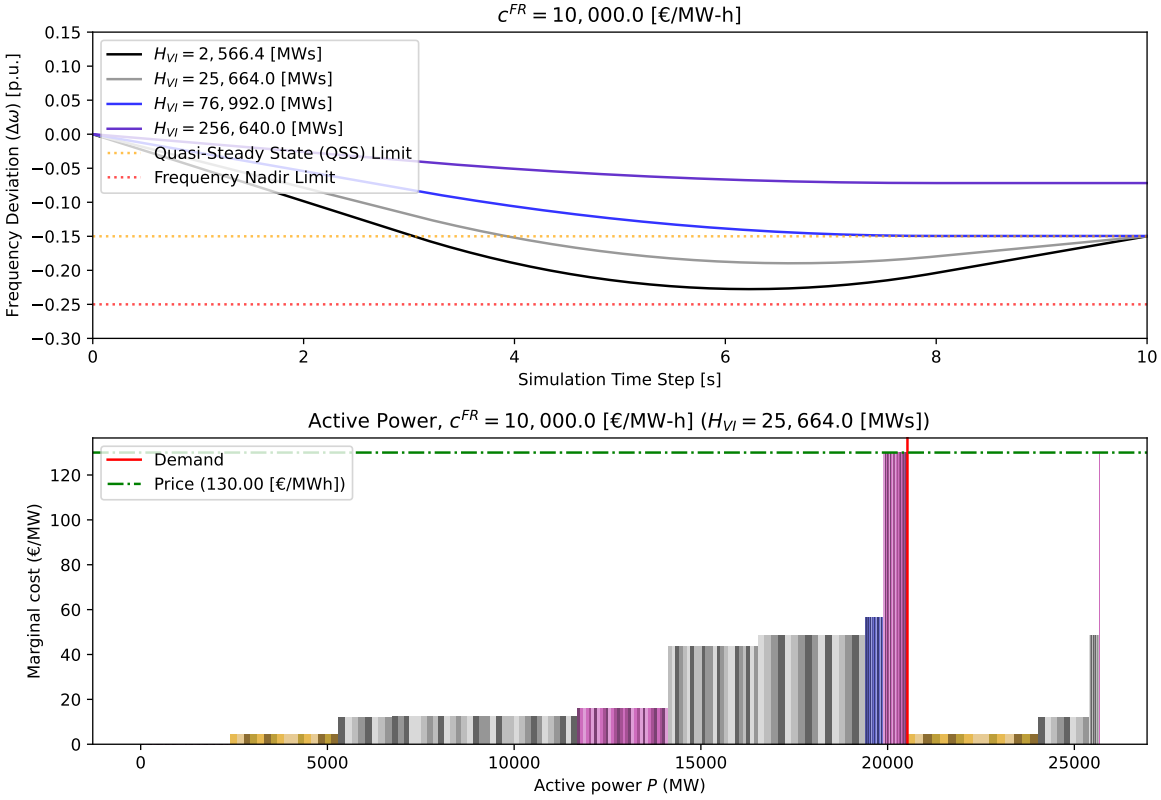

Figure 4.8: Frequency Curve and the Dispatch of Active Power of the Second Sub-Problem When the FR Bid Price is High. The RoCoF is much lower compared to the low-price scenario. This is due to the small value of the largest unit and a larger contribution from the physical inertia by dispatching the active power more evenly among all generation units. The QSS constraint is binding except when the available virtual inertia is very high.

This study case answers the first and the second research question. The amount of FR sold is directly linked to the bid price of FR. The amount of FR sold decreases when the bid price of FR increases. When the frequency nadir constraint is binding, the decrease is continuous and follows the same patterns regardless of the amount of VI available. When the QSS constraint is binding, the decrease is step-wise and the amount of FR stabilizes at a constant level when the price of FR is very high. When the size of the largest unit reaches the maximum possible level, the amount of FR no longer decreases

The size of the largest unit is related to the required FR in a monotonous way according to the formulation of the binding frequency constraint.

4.5. Results of Study Case 2: Dependency Between Amount of VI and Price of VI

Figure 4.9 shows the result of dependency between the amount of VI and the price of VI. In general, the amount of VI decreases with increasing price of VI. However, the curve is not smooth and there are many steps.

The positive correlation between VI and physical inertia implies that VI and physical inertia are not supplementary to each other. The close correlation between VI and the standard deviation of active power and largest power implies that the underlying reason for such dependency is that with higher prices of VI, the optimization problem reduces the size of the largest generation to reduce the demand

for VI to maintain the same level of frequency stability. The positive correlation between VI and the time of frequency nadir shows that the effect of more VI is a slower frequency response, which contributes to the frequency stability.

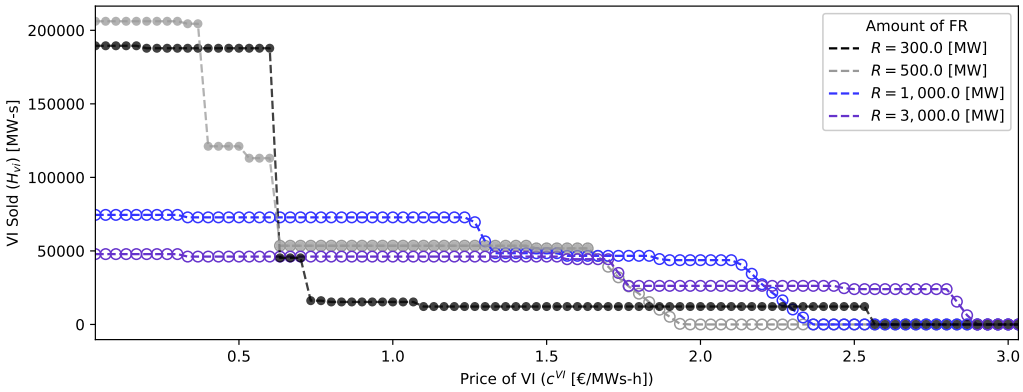

Figure 4.9: Dependency between the amount of VI and the price of VI. When the price of virtual inertia increases, the amount of VI sold decreases in a non-continuous way. When the QSS constraint is binding, the VI decreases in a step-wise way. When the nadir constraint is binding, the VI decreases in a trapezoidal way.

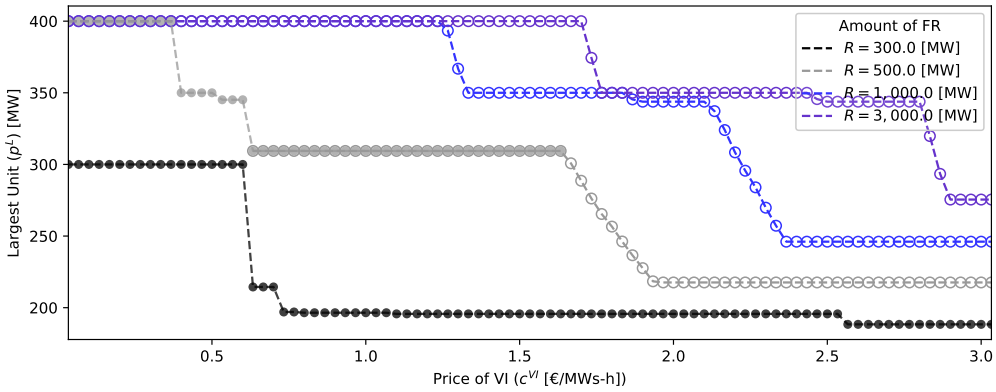

Figure 4.10: Dependency between the size of the largest unit and the bid price of VI.

This study case answers the third research question. The amount of VI decreases when the bid price of VI increases. When the QSS constraint is binding, the decrease is step-wise and when the frequency nadir constraint is binding, the decrease is non-continuous but follows a trapezoidal pattern.

4.6. Result of Study Case 3: Dependency Between the Amount of VI and the Amount of FR

As shown in Figure 4.11, there is no clear pattern of dependency between the amount of VI and the amount of FR. When the price of VI is set at different levels, the curves are different from each other. For each curve, the pattern is not monotonous and thus there is no straightforward explanation of such a pattern.

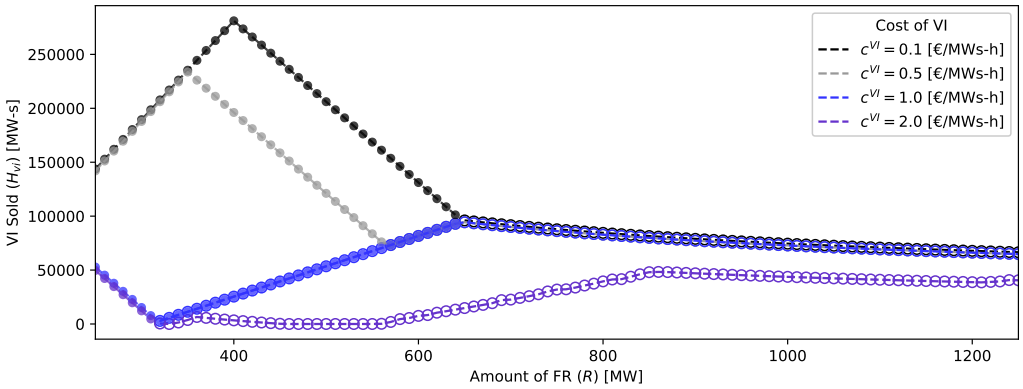

Figure 4.11: The Dependency Between the Amount of VI and the Amount of FR. When there is more FR in the grid, the amount of FR shows different patterns when the price of VI is different. Moreover, the curve of each case is not monotonous.

Figure 4.12 shows the size of the largest unit when the price of VI is set at different levels. The curve for each sub-problem is monotonous.

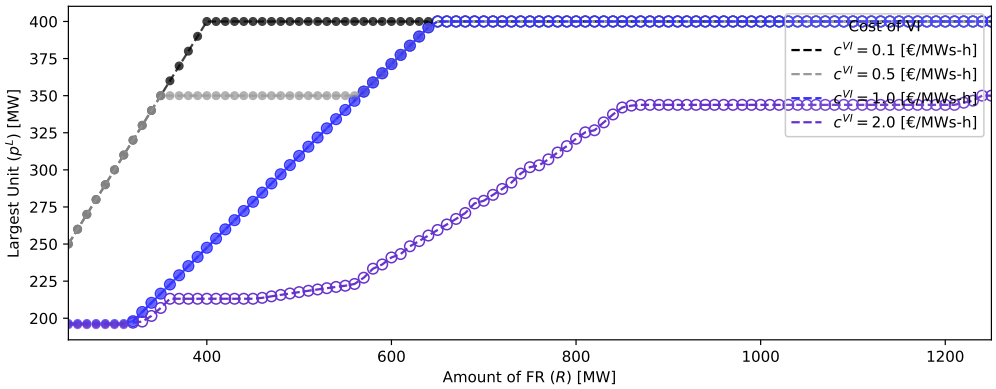

Figure 4.12: The size of the largest unit at different levels of amount of available FR.

This study case answers the fourth research question. The amount of FR sold is not directly related to the amount of VI sold. Other variables need to be taken into consideration when analyzing the pattern.

5

Conclusion

In this project, we proposed a new way to formulate the frequency nadir constraint and a new bid structure for frequency response (FR) and virtual inertia (VI) services in the electricity market. The new bid structure allows providers to bid prices for their provision of FR and VI instead of being assigned shadow prices, as considered in previous works. Each FR bid consists of five parameters, including two parameters describing the dynamics and quality of the FR product, which are the activation delay and the activation speed. Another three parameters of the FR product are the amount of FR, the price per megawatt (MW) of capacity, and a boolean value to indicate whether the bid is flexible and can be partially accepted.

With regards to the modeling of the dynamics of FR products, the linear ramp assumption proposed by Badesa et. al [21, 22, 23] is adopted, which is compatible with different dynamics of FR products. In this project, linear ramps with different parameters are standardized as a curve of the unit capacity, and a binary variable is introduced for FR to indicate whether each FR bid is accepted or not. These two new points coincide with the ideas in the article by George et. al [29].

Three study cases are used to show the patterns of dependencies with the proposed market design, which answers the research questions,

- A1: The amount of FR decreases with the increased bid price of FR almost linearly on the logarithmic scale. This holds when the nadir constraint is binding and the size of the largest unit is not at the maximum level. The curves of the dependency are the same regardless of the available virtual inertia in the grid. The amount of FR stabilizes at a constant level when the FR bid price is very high.
- A2: The size of the largest unit decreases with increasing amount of FR according to the formulation of the binding constraint, which is either nadir constraint or QSS constraint.
- A3: the amount of VI sold decreases with the increasing bid price of VI in a non-continuous way. When the QSS constraint is binding, the decrease is step-wise and when the nadir constraint is binding, the decrease is in a trapezoidal way.
- A4: The amount of VI sold does not have a clear pattern with the amount of FR available.

The results may potentially help understand the basic features of frequency response and virtual inertia market with the bid structure proposed in this project. A complete market mechanism can be

designed based on these features.

The interaction among FR with different dynamics is a topic for future research. The possible gaming opportunities in this bid structure design and possible mitigation methods will be meaningful topics. And it is beneficial to examine the effect of the uncertainty from renewable energy on the identified patterns.

References

[1] Ember. *Denmark electricity generation by source*. 2023. URL: https://ember-climate.org/data/data-tools/data-explorer/ (visited on 09/15/2023).

[2] Benjamin Kroposki et al. “Achieving a 100% Renewable Grid: Operating Electric Power Systems with Extremely High Levels of Variable Renewable Energy”. In: *IEEE Power and Energy Magazine* 15.2 (2017), pp. 61–73. DOI: 10.1109/MPE.2016.2637122.

[3] Ujjwol Tamrakar et al. “Virtual Inertia: Current Trends and Future Directions”. In: *Applied Sciences* 7.7 (June 2017), p. 654. DOI: 10.3390/app7070654. URL: https://doi.org/10.3390%2Fapp7070654.

[4] Padraig Daly, Damian Flynn, and Noel Cunniffe. “Inertia considerations within unit commitment and economic dispatch for systems with high non-synchronous penetrations”. In: *2015 IEEE Eindhoven PowerTech*. IEEE, June 2015. DOI: 10.1109/ptc.2015.7232567. URL: https://doi.org/10.1109%2Fptc.2015.7232567.

[5] Huajie Gu, Ruifeng Yan, and Tapan Kumar Saha. “Minimum Synchronous Inertia Requirement of Renewable Power Systems”. In: *IEEE Transactions on Power Systems* 33.2 (Mar. 2018), pp. 1533–1543. DOI: 10.1109/tpwrs.2017.2720621. URL: https://doi.org/10.1109%2Ftpwrs.2017.2720621.

[6] Erik Ela et al. “Market Designs for the Primary Frequency Response Ancillary Service—Part I: Motivation and Design”. In: *IEEE Transactions on Power Systems* 29.1 (Jan. 2014), pp. 421–431. DOI: 10.1109/tpwrs.2013.2264942. URL: https://doi.org/10.1109%2Ftpwrs.2013.2264942.

[7] Hassan Alsharif, Mahdi Jalili, and Kazi N. Hasan. “Fast frequency response services in low inertia power systems—A review”. In: *Energy Reports* 9 (Oct. 2023), pp. 228–237. DOI: 10.1016/j.egyr.2023.05.193. URL: https://doi.org/10.1016%2Fj.egyr.2023.05.193.

[8] Deven Vatsal, Vivek Sharma, and Kailash Chand Sharma. “Fast Frequency Response Constrained Unit Commitment for Low Inertia Grids”. In: *2023 International Conference on Recent Advances in Electrical, Electronics &; Digital Healthcare Technologies (REEDCON)*. IEEE, May 2023. DOI: 10.1109/reedcon57544.2023.10150820. URL: https://doi.org/10.1109%2Freedcon57544.2023.10150820.

[9] Daniel Fernández-Muñoz et al. “Fast frequency control ancillary services: An international review”. In: *Renewable and Sustainable Energy Reviews* 120 (Mar. 2020), p. 109662. DOI: 10.1016/j.rser.2019.109662. URL: https://doi.org/10.1016%2Fj.rser.2019.109662.

[10] AEMO. *Joint Paper on Essential System Services, Inertia*. Tech. rep. Australia Energy Market Operator, 2022. URL: https://www.aemc.gov.au/news-centre/media-releases/joint-paper-essential-system-services-inertia.

[11] J.W. O’Sullivan and M.J. O’Malley. “A new methodology for the provision of reserve in an isolated power system”. In: *IEEE Transactions on Power Systems* 14.2 (May 1999), pp. 519–524. DOI: 10.1109/59.761875. URL: https://doi.org/10.1109%2F59.761875.

[12] Carmen Cardozo, Laurent Capely, and Philippe Dessante. “Frequency constrained unit commitment”. In: *Energy Systems* 8.1 (Oct. 2015), pp. 31–56. DOI: 10.1007/s12667-015-0166-4. URL: https://doi.org/10.1007%2Fs12667-015-0166-4.

[13] J.W. O’Sullivan and M.J. O’Malley. “Economic dispatch of a small utility with a frequency based reserve policy”. In: *IEEE Transactions on Power Systems* 11.3 (1996), pp. 1648–1653. DOI: 10.1109/59.535710. URL: https://doi.org/10.1109%2F59.535710.

[14] R. Doherty, G. Lalor, and M. O’Malley. “Frequency Control in Competitive Electricity Market Dispatch”. In: *IEEE Transactions on Power Systems* 20.3 (Aug. 2005), pp. 1588–1596. DOI: 10.1109/tpwrs.2005.852146. URL: https://doi.org/10.1109%2Ftpwrs.2005.852146.

[15] Weifeng Li, Pengwei Du, and Ning Lu. “PFR ancillary service in low-inertia power system”. In: *IET Generation, Transmission & Distribution* 14.5 (Feb. 2020), pp. 920–930. DOI: 10.1049/iet-gtd.2019.1536. URL: https://doi.org/10.1049%2Fiet-gtd.2019.1536.

[16] Erik Ela et al. “Market Designs for the Primary Frequency Response Ancillary Service—Part II: Case Studies”. In: *IEEE Transactions on Power Systems* 29.1 (Jan. 2014), pp. 432–440. DOI: 10.1109/tpwrs.2013.2264951. URL: https://doi.org/10.1109%2Ftpwrs.2013.2264951.

[17] Leonard L Grigsby. *Power System Stability and Control (3rd Edition)*. Taylor & Francis Group, 2012.

[18] J.W. O’Sullivan and M.J. O’Malley. “Identification and validation of dynamic global load model parameters for use in power system frequency simulations”. In: *IEEE Transactions on Power Systems* 11.2 (May 1996), pp. 851–857. DOI: 10.1109/59.496165. URL: https://doi.org/10.1109%2F59.496165.

[19] Ti Xu, Wonhyeok Jang, and Thomas Overbye. “Commitment of Fast-Responding Storage Devices to Mimic Inertia for the Enhancement of Primary Frequency Response”. In: *IEEE Transactions on Power Systems* 33.2 (Mar. 2018), pp. 1219–1230. DOI: 10.1109/tpwrs.2017.2735990. URL: https://doi.org/10.1109%2Ftpwrs.2017.2735990.

[20] Ti Xu, Wonhyeok Jang, and Thomas Overbye. “An Economic Evaluation Tool of Inertia Services for Systems with Integrated Wind Power and Fast-Acting Storage Resources”. In: *2016 49th Hawaii International Conference on System Sciences (HICSS)*. IEEE, Jan. 2016. DOI: 10.1109/hicss.2016.307. URL: https://doi.org/10.1109%2Fhicss.2016.307.

[21] Luis Badesa, Fei Teng, and Goran Strbac. “Economic value of inertia in low-carbon power systems”. In: *2017 IEEE PES Innovative Smart Grid Technologies Conference Europe (ISGT-Europe)*. IEEE, Sept. 2017. DOI: 10.1109/isgteurope.2017.8260153. URL: https://doi.org/10.1109%2Fisgteurope.2017.8260153.

[22] L. Badesa, F. Teng, and G. Strbac. “Pricing inertia and Frequency Response with diverse dynamics in a Mixed-Integer Second-Order Cone Programming formulation”. In: *Applied Energy* 260 (Feb. 2020), p. 114334. DOI: 10.1016/j.apenergy.2019.114334. URL: https://doi.org/10.1016%2Fj.apenergy.2019.114334.

[23] Luis Badesa et al. “Assigning Shadow Prices to Synthetic Inertia and Frequency Response Reserves From Renewable Energy Sources”. In: *IEEE Transactions on Sustainable Energy* 14.1 (Jan. 2023), pp. 12–26. DOI: 10.1109/tste.2022.3198324. URL: https://doi.org/10.1109%2Ftste.2022.3198324.

[24] Brent Eldridge, Richard O'Neill, and Benjamin F. Hobbs. "Near-Optimal Scheduling in Day-Ahead Markets: Pricing Models and Payment Redistribution Bounds". In: *IEEE Transactions on Power Systems* 35.3 (May 2020), pp. 1684–1694. DOI: 10.1109/tpwrs.2019.2947400. URL: https://doi.org/10.1109%2Ftpwrs.2019.2947400.

[25] Paul R. Gribik, William W. Hogan, and Susan L. Pope. *Market-Clearing Electricity Prices and Energy Uplift*. Tech. rep. Harvard Electricity Policy Group working paper, 2007. URL: http://www.lmpmarketdesign.com/papers/Gribik_Hogan_Pope_Price_Uplift_123107.pdf.

[26] Gurobi Optimization, LLC. *Gurobi Optimizer Reference Manual*. 2023. URL: https://www.gurobi.com.

[27] Fernando Pérez and Brian E. Granger. "IPython: a System for Interactive Scientific Computing". In: *Computing in Science and Engineering* 9.3 (May 2007), pp. 21–29. ISSN: 1521-9615. DOI: 10.1109/MCSE.2007.53. URL: https://ipython.org.

[28] C. Grigg et al. "The IEEE Reliability Test System-1996. A report prepared by the Reliability Test System Task Force of the Application of Probability Methods Subcommittee". In: *IEEE Transactions on Power Systems* 14.3 (1999), pp. 1010–1020. DOI: 10.1109/59.780914. URL: https://doi.org/10.1109%2F59.780914.

[29] Tim George et al. "Exploring options for new frequency control ancillary service markets in the Australian National Electricity Market". In: *2021 IEEE PES Innovative Smart Grid Technologies - Asia (ISGT Asia)*. IEEE, Dec. 2021. DOI: 10.1109/isgtasia49270.2021.9715660. URL: https://doi.org/10.1109%2Fisgtasia49270.2021.9715660.